Available online at www.sciencedirect.com
ScienceDirect
Palaeogeography, Palaeoclimatology, Palaeoecology 246 (2007) 228–259
PALAEO
www.elsevier.com/locate/palaeo

Holocene sea-level oscillations and environmental changes on the Eastern Black Sea shelf

Elena V. Ivanova [a,*], Ivar O. Murdmaa [a], Andrey L. Chepalyga [b], Thomas M. Cronin [c], Ivan V. Pasechnik [d,1], Oleg V. Levchenko [a], Stephen S. Howe [e], Anastasiya V. Manushkina [d], Elena A. Platonova [d]

[a] *Shirshov Institute of Oceanology, Russian Academy of Sciences, 36 Nakhimovsky Prosp., 117997, Moscow, Russia*
[b] *Institute of Geography, Russian Academy of Sciences, 29 Staromonetny Per., 119017, Moscow, Russia*
[c] *926A National Center US Geological Survey, Reston, Va. 20191, USA*
[d] *Geology Department, Lomonosov Moscow State University, Vorobyevy Gory, 119992, Moscow, Russia*
[e] *Department of Earth and Atmospheric Sciences, ES-351, University at Albany, State University of New York, 1400 Washington Avenue, Albany, NY, USA*

Received 3 November 2005; received in revised form 15 September 2006; accepted 26 September 2006

Abstract

A multi-proxy study of four sediment cores from the Eastern (Caucasian) Black Sea shelf revealed five transgressive–regressive cycles overprinted on the general trend of glacioeustatic sea-level rise during the last 11,000 ^{14}C yr. These cycles are well represented in micro-and macrofossil assemblages, sedimentation rates, and grain size variations. The oldest recovered sediments were deposited in the Neoeuxinian semi-freshwater basin (~10,500–9000 ^{14}C yr BP) and contain a Caspian-type mollusk fauna dominated by *Dreissena rostriformis*. Low δ^{18}O and δ^{13}C values are measured on this species. The first appearance of marine mollusks and ostracodes from the Mediterranean is established in this part of the Black Sea at ~8200 ^{14}C yr BP, i.e., about 1000–2000 yr later than the appearance of marine microfossils in the deeper part of the sea. The Early Holocene (Bugazian to Vityazevian) condensed section of shell and shelly mud sediments with at least two hiatuses represent a high-energy shelf-edge facies. It contains a transitional assemblage representing a mixture of Caspian and Mediterranean fauna. This pattern suggests a dual-flow regime via the Bosphorus after 8200 ^{14}C yr BP. Caspian species disappear and oligohaline species decrease in abundance during the Vityazevian–Prekalamitian cycle. Later, during the Middle to Late Holocene, low sea-level stands are characterized by shell layers, whereas silty mud with various mollusk and ostracode assemblages rapidly accumulated during transgressions. Restricted mud accumulation, as well as benthic faunal composition and abundance, suggest high-energy and well-ventilated bottom water during low sea-level stands. A trend of ^{18}O enrichment in mollusk shells points to an increase in bottom-water salinity during the Vityazevian to Kalamitian transgressions (~7000 to 5700 ^{14}C yr BP) due to a more open connection with the Mediterranean, while a pronounced increase in polyhaline species abundance is established during the Kalamitian to Djemetean transgressions (~6400 to 2700 ^{14}C yr BP). However, the composition of the faunal assemblage indicates that bottom-water salinity never exceeded modern values of 18–20 psu.

Keywords: Black Sea; Transgression; Regression; Cycles; Holocene; Macro- and microfossils; Caucasian shelf; Paleoenvironments; Abrupt changes

* Corresponding author. Tel.: +7 495 129 2163; fax: +7 495 124 5983.
E-mail address: e_v_ivanova@ocean.ru (E.V. Ivanova).
[1] Present address: WesternGeco/Schlumberger, Suite 2300, 645 — 7th Avenue N.W., Calgary, AB, Canada, T2P 4G8.

0031-0182/$ - see front matter © 2006 Elsevier B.V. All rights reserved.
doi:10.1016/j.palaeo.2006.09.014

1. Introduction

It is generally established that global sea level rose from a lowstand somewhere between ~135 m and 110 m at 18,000 ^{14}C yr BP (Fairbanks, 1989). However, sea-level oscillations for several semi-closed basins, such as the Black Sea (Fedorov, 1978; Chepalyga, 2002), have shown a punctuated character. Transgressions (high stands) of the Black Sea level were suggested by Andrusov nearly 100 yr ago (see Andrusov, 1965), and confirmed by later studies of marine terraces, in particular on the Caucasian coast where higher than present level was established at ~6000 ^{14}C yr BP (Fedorov, 1985; Balabanov and Izmailov, 1988). Low stands in sea level are poorly known, however, because they are not exposed in coastal outcrops and may only be studied using sediment cores taken below present sea level. Moreover, the succession of level oscillations in the Black Sea has to be interpreted in conjunction with the timing of its final inundation by Mediterranean waters during the Early Holocene, between 9000 and 7000 ^{14}C yr BP (Ross and Degens, 1974; Ryan et al., 1997; Ballard et al., 2000; Uchupi and Ross, 2000; Chepalyga, 2002; Kaplin and Selivanov, 2004). Despite these studies, the exact timing and pattern of the Early Holocene sea level rise and the flooding of the Black Sea is still disputable.

In this paper, we focus on unresolved problems of sea-level and salinity variations during the Holocene using paleontological, paleoecological, sedimentological, geochemical, and seismostratigraphic evidence, and ^{14}C-dates, obtained on the Eastern (Caucasian) shelf, from 55 to 101 m below modern sea level.

Specifically, we will address the following questions:

1. How did the transgressive–regressive cycles associated with sea-level changes influence faunal assemblages at different water depths on the outer shelf?
2. How did different benthic faunal groups (mollusks, ostracodes, foraminifers) respond to changes in hydrodynamics, bottom water ventilation, salinity, sedimentation rates, and other environmental characteristics related to the opening of the marine connection with the Mediterranean?
3. Are high and low sea-level stands identified by changes in faunal assemblages also reflected in variations in sedimentary facies and seismic patterns?
4. Is there evidence of the regional sea-level regressions referred to as the Phanagorian (~2700–2300 cal yr BP; Fedorov, 1978) and the Kundukian (4400–4100 ^{14}C yr BP; Chepalyga, 2002) on the shelf?

2. Area description, methods, and material studied

2.1. Material

Four gravity cores were retrieved from the Eastern (Caucasian) Black Sea shelf, during cruise 27 by RV *Akvanavt* in 2001 (Fig. 1), along high-frequency CHIRP-sonar seismic profiles (Figs. 2 and 3). Cores Ak 521 (44°15.41′ N, 38°32.26′ E, water depth 101 m) and Ak 522 (44°15.58′ N, 38°32.30′ E, water depth 93 m) were collected from the outer shelf off the Arkhipo–Osipovka village. Cores Ak 497 (44° 32.43′ N, 37°57.31′ E, water depth 55 m) and Ak 500 (44°32.02′ N, 37°56.97′ E, water depth 71 m) were obtained from the outer shelf and upper continental slope off the town of Gelendjik (Murdmaa et al., 2003).

2.2. Methods

2.2.1. High-frequency seismic profiling

A high-resolution survey of the structure of the bottom sediments was conducted during the RV *Akvanavt* 2001 cruise using a CHIRP-II (Datasonics Inc.) sub-bottom profiler (2–7 kHz) with an electrical pulse power of 4 kW and a shooting interval of 0.25 s. The TTV-190 vehicle was towed at a depth of 5–15 m with the ship speed of 4 knots. The position of the vessel was determined using a differential global positioning system to an accuracy better than 5 m. The sound velocity is taken equal to 1500 m/s both for water and sediments. The error in thickness owing to velocity deviation does not exceed 0.01 m.

2.2.2. Micro- and macrofossil analyses

The cores were sampled at 2- to 20-cm intervals and sieved through a 125 μm mesh using distilled water. The sediment fraction >125 μm was investigated under a binocular microscope for planktic and benthic foraminifers (core Ak 521), ostracodes (cores Ak 521, Ak 522, and Ak 500), and mollusks (all cores) (Appendix, Tables A1–A9). Fractions with very abundant microfossils were split to obtain sufficient numbers of microfossils and mollusk shells to characterize the assemblages. Generally, 200 to 400 foraminiferal tests and 50 to 200 ostracode shells were identified and counted at a species level where possible. The total number of ostracode specimens identified in every sample and percentages of species are given in (Appendix, Tables A5–A7).

2.2.3. Stable isotope measurements

The stable isotopic composition of shells from five species, *Cardium exiguum, Modiolus phaseolinus,*

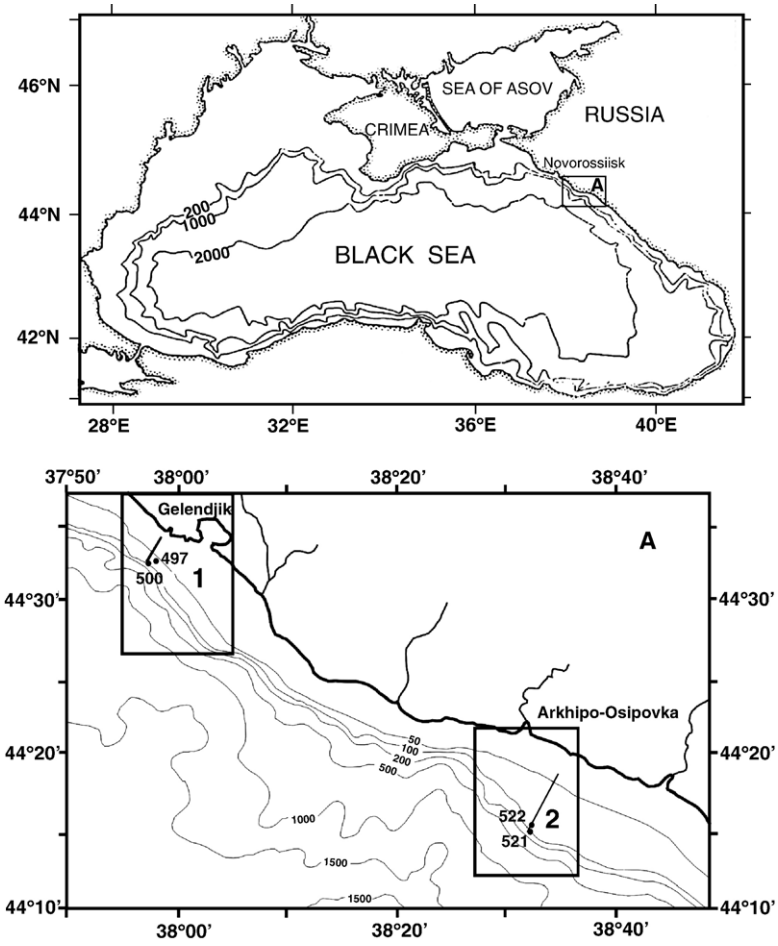

Fig. 1. Location map of the Black Sea. Inset of the study area (A) illustrates the location of two seismic profiles (solid lines) and gravity cores (circles) recovered during cruise 27 by the RV *Akvanavt*. Water depth isopleths in meters.

Mytilaster lineatus, Mytilus edulis, and Dreissena rostriformis, were analyzed from cores Ak 500 and Ak 521 due to an insufficient number of shells from any single species. Each sediment horizon was generally 2–6 cm thick and generally yielded 2–5 shells of one or two species (Appendix, Tables A10 and A11).

The shells were cleaned in deionized water in an ultrasonic bath for several minutes and dried overnight at 60 °C. The dried shells were then cut approximately in half subparallel to the axis of maximum growth from umbo to ventral margin, and one half was processed further for isotopic analysis.

Preliminary analyses indicated that the carbon and oxygen isotopic compositions of periostracum-coated *Modiolus* shell were up to 0.5‰ more depleted than shell with the periostracum removed, contrary to the findings of Vander Putten et al. (2000) for *Mytilus*. In addition, the carbon and oxygen isotopic compositions of the outer calcitic layer of *Mytilus* were found to be up to 2‰ more depleted than those of the inner aragonitic layer. For these reasons, and because of a lack of consensus concerning the likelihood of altering the isotopic compositions of the shell during removal of organic matter from the periostracum by soaking in either dilute sodium hypochlorite (Keatings et al., 1999) or hydrogen peroxide (Gaffey and Bronnimann, 1993), or by roasting *in vacuo* (Grossman, 1982; Grossman et al., 1986), shell material was separated physically using extremely sharp, thin knife blades and probes.

Half-shells of *Cardium* and *Dreissena* were powdered in an agate mortar and pestle without additional separation, whereas half-shells of *Modiolus, Mytilaster, and Mytilus* required further preparation. The periostracum was carefully removed from the underlying calcium carbonate of half-shells of *Modiolus* and *Mytilaster*, while half-shells of *Mytilus* were carefully separated between the periostracum-

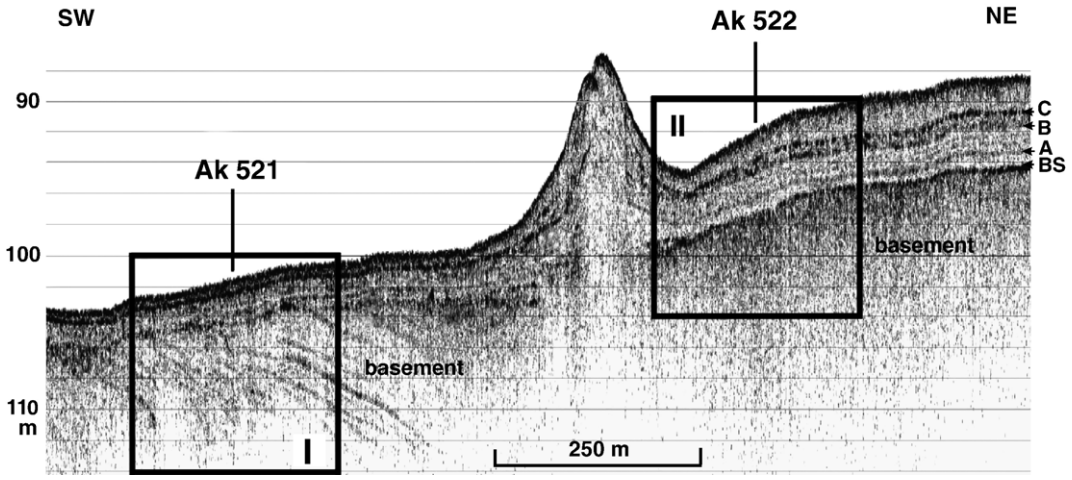

Fig. 2. Seismic profile across the outer shelf off the Arkhipo–Osipovka village showing locations of cores Ak 521 and Ak 522 and reflectors A, B, B_1, and BS (see text for explanation). Fragments of seismic records at coring sites are shown on Figs. 5(I) and 6(II) respectively.

coated outer calcitic layer and the periostracum-free inner aragonitic layer. The periostracum-free portions of these shells were then powdered in an agate mortar and pestle.

Approximately 200 μg of powdered shell was dissolved in 100% phosphoric acid at 90 °C in individual reaction vessels in a MultiPrep sample preparation device, and the evolved CO_2 gas was analyzed using a Micromass Optima gas-source triple-collector isotope ratio mass spectrometer at the University at Albany, State University of New York. Samples of international standard NBS-19 were interspersed among the shell samples in analytical runs.

All carbon and oxygen isotopic compositions are reported as per mil (‰) deviations relative to Vienna Peedee belemnite (VPDB). The average isotopic compositions and standard deviations of 29 samples of NBS-19 were $\delta^{13}C = 1.949 \pm 0.013$‰ and $\delta^{18}O = -2.204 \pm 0.030$‰. The average difference between the 25 replicate mollusk samples analyzed from core Ak 521 was 0.122‰ for $\delta^{13}C$ and 0.051 for $\delta^{18}O$ and

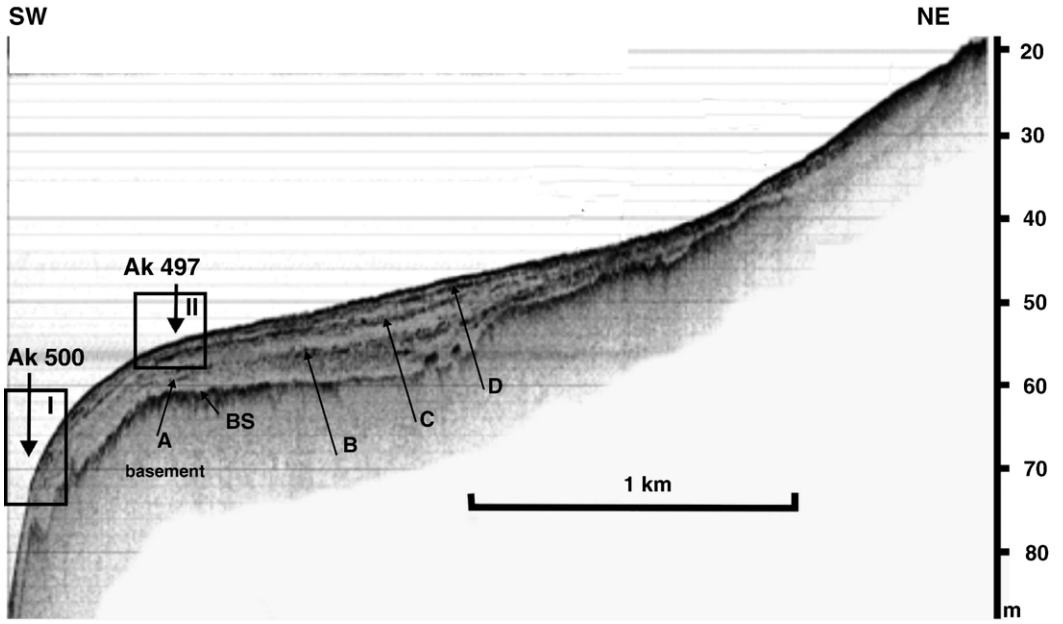

Fig. 3. Seismic profile across the shelf off the town of Gelendjik showing locations of cores Ak 500 and Ak 497 and reflectors A, C, D, and BS (see text for explanation). Fragments of seismic records at coring sites are shown on Figs. 7(I) and 8(II) respectively.

Table 1
AMS-^{14}C dates

Lab code	Core	Depth in core (cm)	Mollusk species	Conventional 14C age (yrs BP)
Beta 205453	Ak 521	24–26	*Mytilus edulis*	4440±40
Beta 205454	Ak 521	31–34	*Mytilus edulis*	5750±40
OS 36729	Ak 521	51–54	*Mytilus edulis*	6020±30
OS 36653	Ak 521	102–107	*Mytilus edulis*	6420±45
OS 36651	Ak 500	44–46	*Mytilus edulis*	1080±45
OS 36654	Ak 500	134–136	*Cardium exiguum*	2730±40
Beta 205452	Ak 500	199–200	*Cardium exiguum*	2170±40

between the 10 replicate samples from Ak 500 was 0.090‰ for δ^{13}C and 0.079‰ for δ^{18}O. The isotopic compositions of 138 shells sampled from multiple-shell horizons from Ak 521 were later averaged after combining the analyses into 60 monospecific groups, as were the compositions of 66 shells from Ak 500 after combining into 27 groups, in order to present the isotopic data graphically with greatest clarity. The average of the standard deviations of the isotopic compositions within these sample clusters was 0.307‰ for δ^{13}C and 0.108‰ for δ^{18}O for core Ak 521, and 0.292‰ for δ^{13}C and 0.147‰ for δ^{18}O for Ak 500.

2.2.4. Radiocarbon dating

The chronology of the cores is based on seven AMS ^{14}C dates (Table 1) and twelve radiometric dates (Table 2). AMS ^{14}C were carried out at NOSAMS, Woods Hole Oceanographic Institution, and at Beta Analytic. Small monospecific samples of 9–12 g pure $CaCO_3$ were cleaned in an ultrasonic bath with distilled water for 5 to 10 min. Normally, one shell of *Mytilus edulis* of >0.5 cm length or 1–2 shells of *Cardium exiguum* were sufficient for analysis. Radiometric dates were obtained on large samples of mollusk shells at the Laboratory of Isotope Geochemistry of Geological Institute, Russian Academy of Sciences. Sediment layers 5- to 10-cm-thick (about 100 g) and enriched in large shells of bivalves and gastropods were selected. The shells were treated with HCl before the measurements. Measured ages were converted to conventional ages by applying a δ^{13}C correction of 0–1‰ obtained at NOSAMS and Beta Analytic during AMS ^{14}C measurements.

3. Results

3.1. Lithology and stratigraphy

Previously established stratigraphy of the Late Glacial to Holocene sediments of the Northern and Eastern Black Sea (from Bulgarian to Georgian coast) is based on the study of molluscan assemblages from the shelf, coastal and terrace sediments (Nevesskaya,

Table 2
Radiocarbon dates

Lab code GIN RAS	Core	Depth in core (cm)	Material	Conventional ^{14}C age (yr BP)*
INN 12063 a	Ak 521	148–158	Mixed bivalve shells	6920±100
INN 11848	Ak 521	158–168	Mixed bivalve shells	8180±100
INN 11937	Ak 521	175–185	Mixed bivalve shells	8150±110
INN 11938	Ak 521	185–195	Mixed bivalve shells	8500±110
INN 11849	Ak 521	195–200	Mixed bivalve shells	10,450±190
INN 12061	Ak 522	119–125	Mixed bivalve shells	4350±100
INN 12062	Ak 522	135–139	Mixed bivalve shells	4960±100
INN 12063	Ak 522	191–195	Mixed bivalve shells	5570±120
INN 11846	Ak 500	104–109	Mixed bivalve shells	2770±80
INN 12058	Ak 497	66–69	Mixed bivalve shells	2260±60
INN 12059	Ak 497	69–71	Mixed bivalve shells	2630±100
INN 12060	Ak 497	71–74	Mixed bivalve shells	2410±100

Notes: * Conventional ages were estimated applying the δ^{13}C correction 0–1‰ according to values obtained during AMS ^{14}C measurements in the same sediment cores (see Table 1).

1965; Fedorov, 1977; Chepalyga et al., 1989), and on benthic foraminifers and ostracodes from deep-sea cores and coastal sequences (Yanko, 1982, 1989; Yanko and Gramova, 1990). We use here the recent regional stratigraphic scheme by Chepalyga (2002), which is based on the well-established succession of the Black Sea level oscillations (high and low stands) and corresponding sediment layers with faunal assemblages, inferred from both coastal and marine data. Unfortunately, the timing of the boundaries between the traditional Black Sea stratigraphic units, as well as the amplitude of corresponding sea-level oscillations, especially of low stands, is still disputable, especially prior to the archeologically dated Phanagorian low-stand event, although numerous ^{14}C (mainly uncorrected) dates have been obtained in the region (e.g., Arslanov et al., 1982; Balabanov and Izmailov, 1988; Kaplin and Selivanov, 2004; Izmailov, 2005). As our material is insufficient to precisely date unit boundaries, they are drawn in Fig. 4 by interpolating between dated high and low sea-level stands.

3.1.1. Seismic stratigraphy

The seismic profiles (Figs. 2 and 3) demonstrate a sedimentary sequence, 2–10 m thick, concordant to the bottom surface and gently dipping seaward across the narrow (4–10 km wide) shelf. The sediment cover unconformably overlies the acoustic basement (BS), made up of the folded Cretaceous–Paleogene flysch. A regional reflector (A) is traced in seismic profiles across the shelf and is recovered by core Ak 521 (Fig. 5), where it corresponds to the lower shell layer or the hiatus within this layer at about 2 m below sea floor (1 m above the BS). Its age of ~10,000–9000 ^{14}C yr BP (stratigraphically above the sample ^{14}C-dated at 10,450±190 yr BP) roughly corresponds to the Neoeuxinian–Bugasian transition (Fig. 4). The reflector *A* is also well delineated at the site of core Ak 522 (Fig. 6). At the shallower shelf edge off Gelendjik (about 60–70 m), the same, but possibly somewhat younger, reflector overlies a transparent seismic unit that smoothes the eroded basement surface at Ak 500 (Fig. 7).

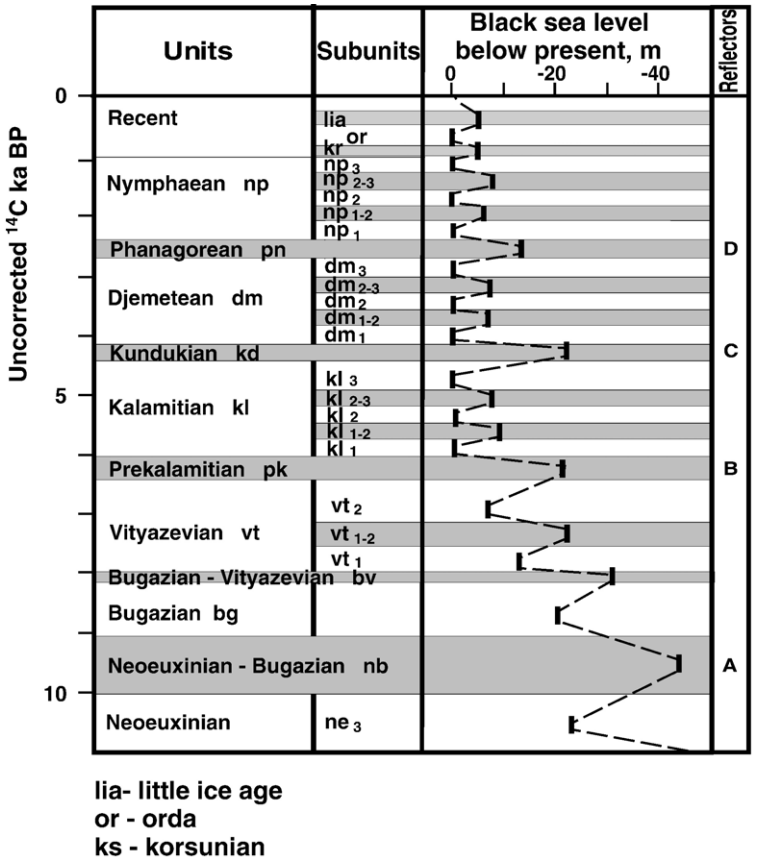

Fig. 4. Stratigraphic scheme with corresponding Black Sea level high and low stands (modified from Chepalyga, 2002). The position of seismic reflectors A–D is shown.

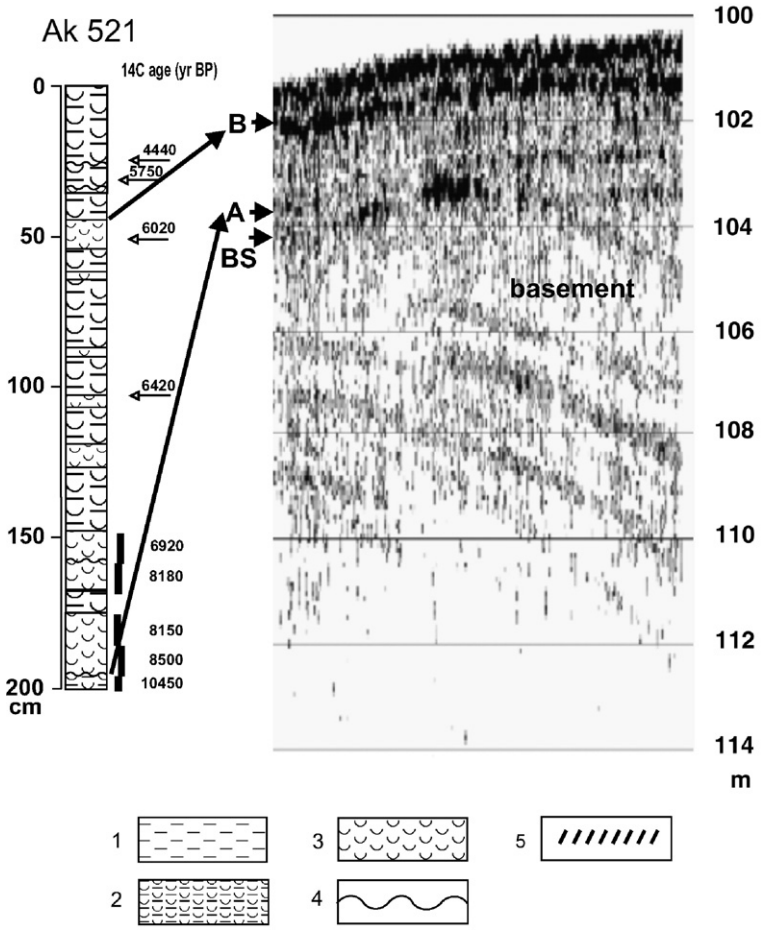

Fig. 5. Core Ak 521 with the corresponding portion of seismic profile. Arrows show the correlation of core records with seismic reflectors. Lithology: (1) silty mud with rare small mollusk shells and their fragments, (2) muddy shell layers (or shelly mud) with almost equal content of shells and mud; (3) shell layers with minor mud content, (4) hiatus, and (5) angular unconformity.

The overlying thinly stratified, about 1.5 m thick, seismic unit in the SE profile (Fig. 2) corresponds to the interval ca. 150–50 cm in core Ak 521 (Fig. 5) composed of interbedded shell and shelly mud layers. The same unit is directly traced to station Ak 522, where its thickness is almost 2 m. However, it is poorly expressed in the seismic profile off Gelendjik (Fig. 3). A rather strong reflector B at the top of the unit possibly corresponds to a sharp decrease in sedimentation rate or a hiatus, related to the termination of rapid sediment accumulation at about 6000 ^{14}C yr BP (Fig. 5). Between stations Ak 521 and Ak 522 the reflector bifurcates (Fig. 2). Both reflectors B and C are presumably recovered by core Ak 522, where they correspond to muddy shell layers (Fig. 6).

The sediment cover above the basement is 9 m thick at site Ak 500, where an erosional channel underlies the marine sediment cover (Fig. 7), and it is 6 m thick at site Ak 497 in the outer shelf off Gelendjik (Fig. 8). Note, both stations Ak-500 and Ak-497 are not exactly located at the location map shown in Fig. 1, and we plotted these core sites on the profile (Fig. 3) based on their actual water depth. Strong reflector C is recovered at the bottom of core Ak 497 as a shell layer (Fig. 8) presumably formed during the Kundukian regression (Fig. 4). The indistinct reflector D between C and the acoustic basement in core Ak 497 (Fig. 8) and reflector D_1 in core Ak 500 (Fig. 7) correlate with shell layers corresponding to the Phanagorian regression, according to radiocarbon dates (Tables 1 and 2, Fig. 4), but the upper layer is likely reworked from the shelf edge.

3.1.2. Lithostratigraphy, chronostratigraphy, and sedimentation rates

Sediments in all four cores are composed of olive gray to dark olive gray terrigenous silty mud and

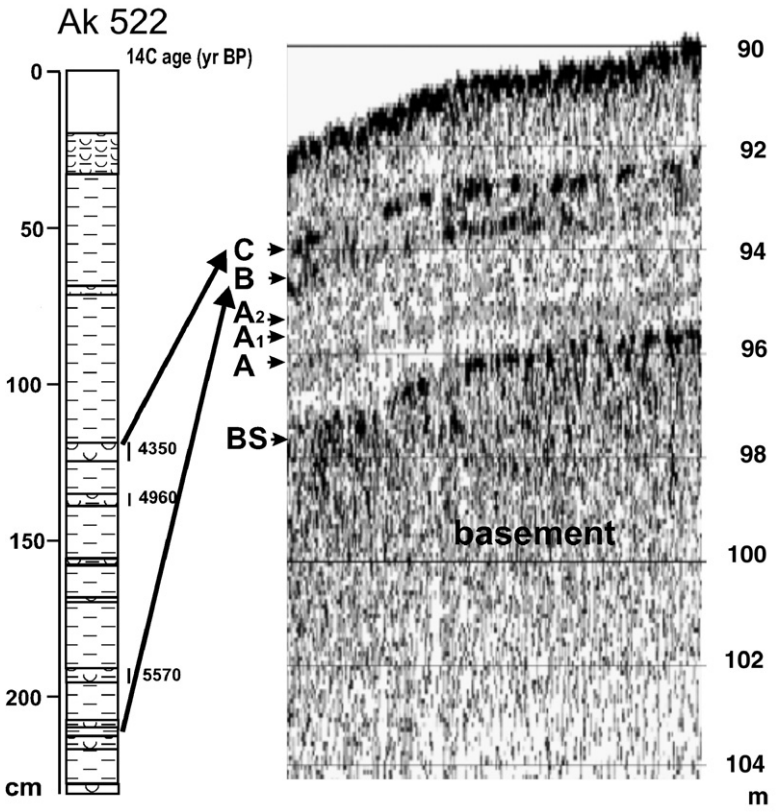

Fig. 6. Core Ak 522 with the corresponding fragment of seismic profile. Arrows show correlation of core records with seismic reflectors (see Fig. 5 for lithologic symbols).

bivalve shells or shell fragments from sand-size to several centimeters in diameter. The cores recovered sediment ranging from silty mud almost barren of shells to concentrated shell layers with minor mud content. The sediments were subdivided into three types according to shell content: (1) silty mud with rare small mollusk shells and their fragments, containing less than 10% of fractions coarser than 0.1 mm; (2) muddy shell sediment (or shelly mud) with 10–50% of coarse fractions (>0.1 mm) composed of shell carbonate; and (3) shell layers with more than 50% of fractions coarser than 0.1 mm.

The reference core Ak 521 (Fig. 5) penetrated the entire Holocene section and recovered the top of Upper Pleistocene (Neoeuxinian) deposits. The lithology of the core is characterized by multiple alternations of two sediment types: a shell layer and a shelly mud with variable, but locally abundant, bivalve shells. The thickness of individual layers varies from 1–2 cm to 20–35 cm. The proportion of shell layers increases downward, especially below 120 cm, whereas the upper part is dominated by shelly mud with more rare and thinner (2–3 cm) shell layers.

The basal Neoeuxinian layer consists of shelly mud with a ^{14}C-date of 10,450±190 yr BP (Table 2). It is overlain by two 20-cm-thick shell layers with a shelly mud interbed, likely separated from the basal shelly mud by more than a 1000-year-long hiatus. According to four ^{14}C dates, the 50-cm-thick shell deposit spans a time interval from 8500 to 6900 ^{14}C yr BP and accumulated at an average rate of 31 cm/ka (Fig. 9). Together with the hiatus at the base, it roughly corresponds to Bugasian and Vityazevian stages (Fig. 4).

The overlying sequence of alternating shell and shelly mud layers, more than 1 m thick (Fig. 5), accumulated during about 1000 yr (6900–5800 ^{14}C yr BP) with linear sedimentation rates of 70–128 cm/ka (Fig. 9). We suggest that this interval belongs to the Prekalamitian–Kalamitian transgression and the following high sea level stand (Fig. 4). Sedimentation rates decreased after 6000–5800 ^{14}C yr BP and one or more hiatuses possibly occur in the upper part of the Kalamitian interval, which terminated with the pronounced Kundukian regression marked by a shell layer at 32 cm below the sea floor. The average linear sedimentation rate for the core top is very low

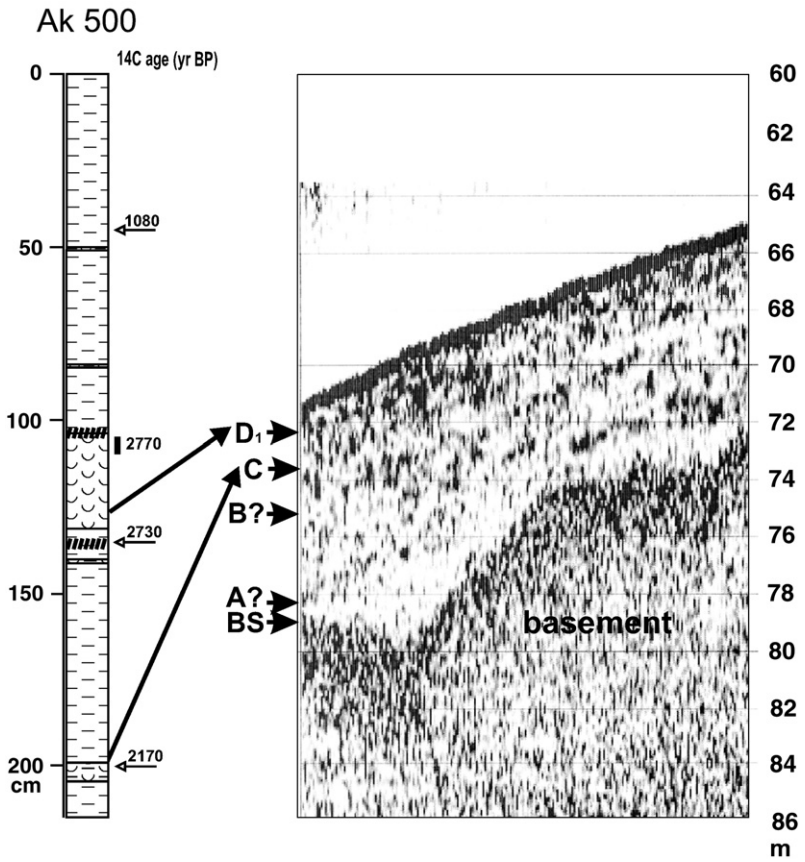

Fig. 7. Core Ak 500 with the corresponding fragment of seismic profile. Arrows show correlation of core records with seismic reflectors (see Fig. 5 for lithologic symbols).

(5.7 cm/ka), possibly due to a hiatus (or even erosion?) related to the Kundukian and/or Phanagorian regression.

Core Ak 522 (Fig. 6) is also composed of alternating mud and shell layers, but differs from the above described core Ak 521 in its less abundant shell content. ^{14}C dates (Table 2) suggest that silty mud with thin muddy shell layers accumulated rapidly (about 90 cm/ka) upward to the ^{14}C date of 4960± 100 yr BP (Fig. 9). The Kalamitian mud layer is overlain by the Kundukian shell layer dated by 4350± 100 yr BP. A distinct facies change from the "mytilus mud" below to the "phaseolina mud" above coincides with this regression (see following section), whereas the phaseolina mud belongs to the Djemetean high sea level stand. A shell layer occurs at the core top that possibly corresponds to the Phanagorian regressive phase. About 20 cm of mud from the top were lost during coring.

Cores Ak 500 (Fig. 7) and Ak 497 (Fig. 8) from the uppermost continental slope and outer shelf off Gelendjik, respectively, consist mainly of silty mud with rare mollusk shells and a minor proportion of muddy shell layers. Core Ak 500 is comprised of two distinct muddy shell interbeds. The lower shell layer is likely related to the Phanagorian regression according to the AMS-^{14}C date of 2170±40 yr BP (at 199–200 cm), although the date is somewhat younger than that commonly accepted for the termination of the Phanagorian event (~2300 yr BP, Fig. 4). A sharp oblique contact separates the upper muddy shell layer from the underlying mud. Two ^{14}C dates (2730±40 and 2770±80) also indicate the Phanagorian regression deposit (Tables 1 and 2). The inversion of ^{14}C dates in the core and the angular discontinuity at the upper shell layer base point to its reworked origin. A muddy shell layer recovered at the bottom of core Ak 497 most likely correlates with the Kundukian regression. Three dates in the upper muddy shell layer (within 2700–2200 ^{14}C yr BP, with the inversion of two dates almost within±100-year error of measurements, Table 2, Fig. 8) suggest that it was

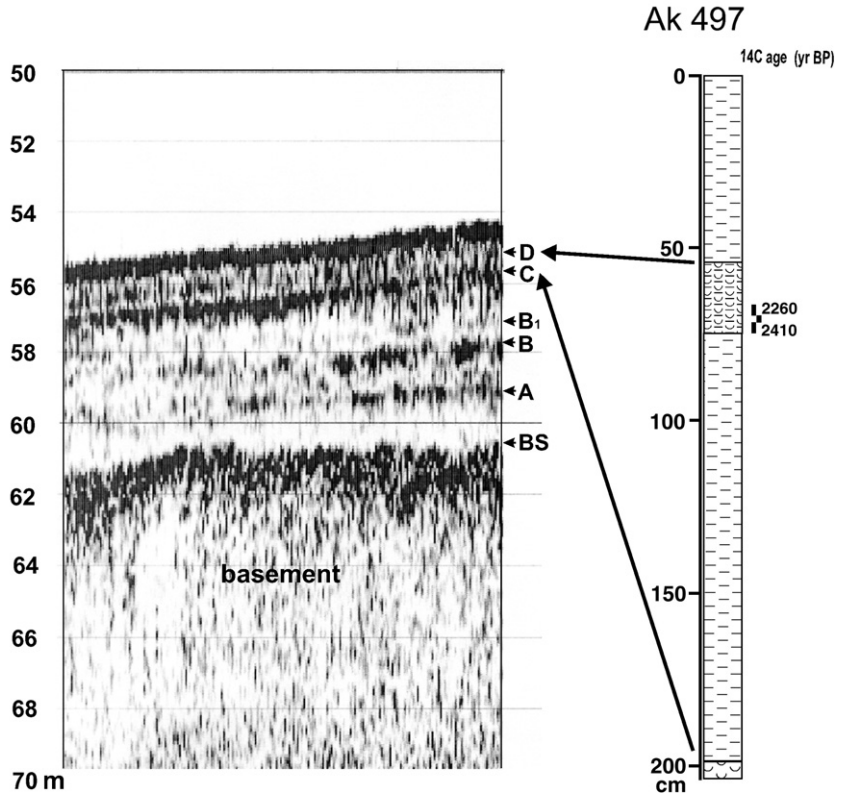

Fig. 8. Core Ak 497 with the corresponding fragment of seismic profile. Arrows show correlation of core records with seismic reflectors (see Fig. 5 for lithologic symbols).

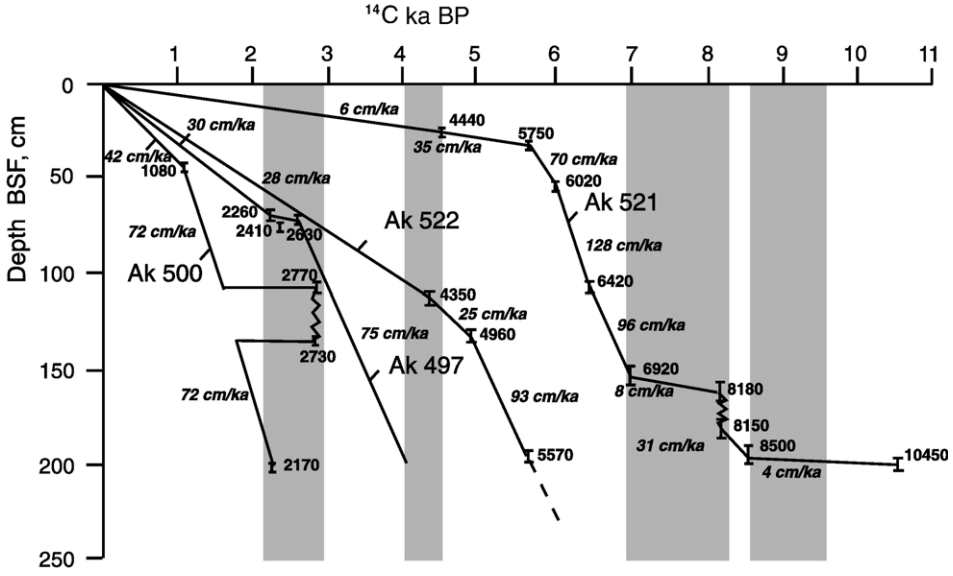

Fig. 9. Linear sedimentation rates between ^{14}C dates. Dated intervals are shown by solid bars with conventional ages, the inclination of thin lines indicates linear sedimentation rates, while the extrapolation of sedimentation rates below dates and the inversion of dates are shown by dashed and sawtooth lines, respectively.

formed during the Phanagorian regression. The Djemetean silty mud between the assumed Kundukian and dated Phanagorian shell layers in core Ak 497 accumulated at a rate about 70 cm/ka, whereas moderate sedimentation rates (30–40 cm/ka) characterize the Nymphaean to Recent mud accumulation in both cores (Fig. 9).

3.2. Macro-and microfossil

3.2.1. Mollusks

Several molluscan assemblages identified in our cores (Appendix, Tables A1–A4) are known to characterize different depositional paleoenvironments. A semi-freshwater (or demi-freshwater according to Chepalyga (2002)) assemblage, found only in the lowermost part of core Ak 521 from 200 to 168 cm (Fig. 10), in the condensed Neoeuxinian to Early Vityazevian layer, is enriched in mollusk and gastropod shells. The assemblage contains endemic Caspian species: *Dreissena rostriformis*, *Monodacna caspia*, *Theodoxus pallasi*, *Micromelania* sp. Neither freshwater nor marine species occur in the assemblage which points to bottom-water salinity of about 2 to 8 psu. Caspian species penetrated into the Black Sea via the Manych Strait much earlier, at ~16,000–14,000 ^{14}C yr BP (Chepalyga, 2002).

A transitional assemblage of Vityazevian character occurs in the interval 168–148 cm in Core Ak 521 (Fig. 10) and represents a mixture of the Caspian species noted above and marine Mediterranean species that include *Mytilus edulis*, *Ostrea edulis*, *Cardium edule*, and *Corbula gibba*. The latter two species are typical for Vityazevian sediments (Nevesskaya, 1965) and appeared in core Ak 521 at ~8200 ^{14}C yr BP. The upward disappearance of Caspian fauna and increase in marine species indicate that salinity rose during the Vityazevian transgression.

A *Mytilus* mud assemblage found at several levels in all cores (Figs. 10–13) provides evidence for high variability in species diversity and abundance. Generally, the whole shells and fragments of adult *Mytilus edulis* strongly dominate this assemblage like in Prekalamitian to Kalamitian sediments of cores Ak 521 and Ak 522. However, at some levels in other cores *Cardium exiguum*, *Modiolus adriaticus* or *Bittium reticulatum* become even more abundant. The number of species reaches 8 to10 in the most diverse *Mytilus* mud assemblage from lower Nymphaean sediments in core Ak 500 (199–136 cm) decreasing upward in cores Ak 500 and Ak 497. Several shells of *D. rostriformis* are found within this assemblage from the lower Prekalamitian sediments in Core Ak 521, perhaps due to the longer survival of the species in the Black Sea compared to other Caspian fauna. Alternatively, *D. rostriformis* may be reworked from Vityazevian layer with its transitional assemblage. The species in the assemblage (like *Cardium exiguum*, *C. paucicostatum*, *Retusa truncatula*) point to relatively deep-water environments with moderate salinity (15–20 psu), whereas a considerable number of juveniles at several horizons indicates rather slow bottom currents and low oxygen content.

The *Mytilus* bank assemblage differs from the previous one by a much greater abundance of whole shells, juveniles and fragments of *M. edulis*. In general, it is almost a monospecific assemblage occurring in 20–30 cm-thick shell layers at different levels in all cores (Figs. 10–13). The most diverse *Mytilus* bank assemblage corresponds to the Phanagorian layer in cores Ak 497 and Ak 500 (reworked) (Figs. 12 and 13) where it contains up to 11–13 species with *C. paucicostatum* being the most abundant at some levels. This diverse assemblage supports the presence of a well-ventilated relatively shallow marine basin with intense bottom water hydrodynamics, according to studies of similar modern fauna (Nevesskaya, 1965; Kiseleva, 1981).

The diverse *Modiolus phaseolinus* mud assemblage is limited to the Djemetean layer in core Ak 522 (Fig. 11) and resembles the well-known “phaseolina mud” on the Recent outer shelf described by Arkhangelskii and Strakhov (1938) near Odessa. The dominance of *M. phaseolinus* and absence of several other species point to low temperature, slow bottom currents and poor ventilation at water depth of ~90 m.

The *Modiolus phaseolinus* bank assemblage in core Ak 522 (Fig. 11) differs from the previous one by a much greater abundance of shells in the sediment and lower species diversity. Most likely it developed during the Phanagorian regression and reflected active hydrodynamics and a moderate dissolved oxygen content.

A shallow-water assemblage is found only in the lower part of core Ak 497, in the Djemetean layer (Fig. 13). It is represented by *C. exiguum* and *Cerithium vulgatum*, among other species, which allow us to assume stressful conditions with moderate oxygenation of bottom water.

A sparse relatively deep-water assemblage with a low number of shells characterizes Nymphaean to Recent sediments except in core Ak 522 where this time interval was not recovered. It contains rare shells

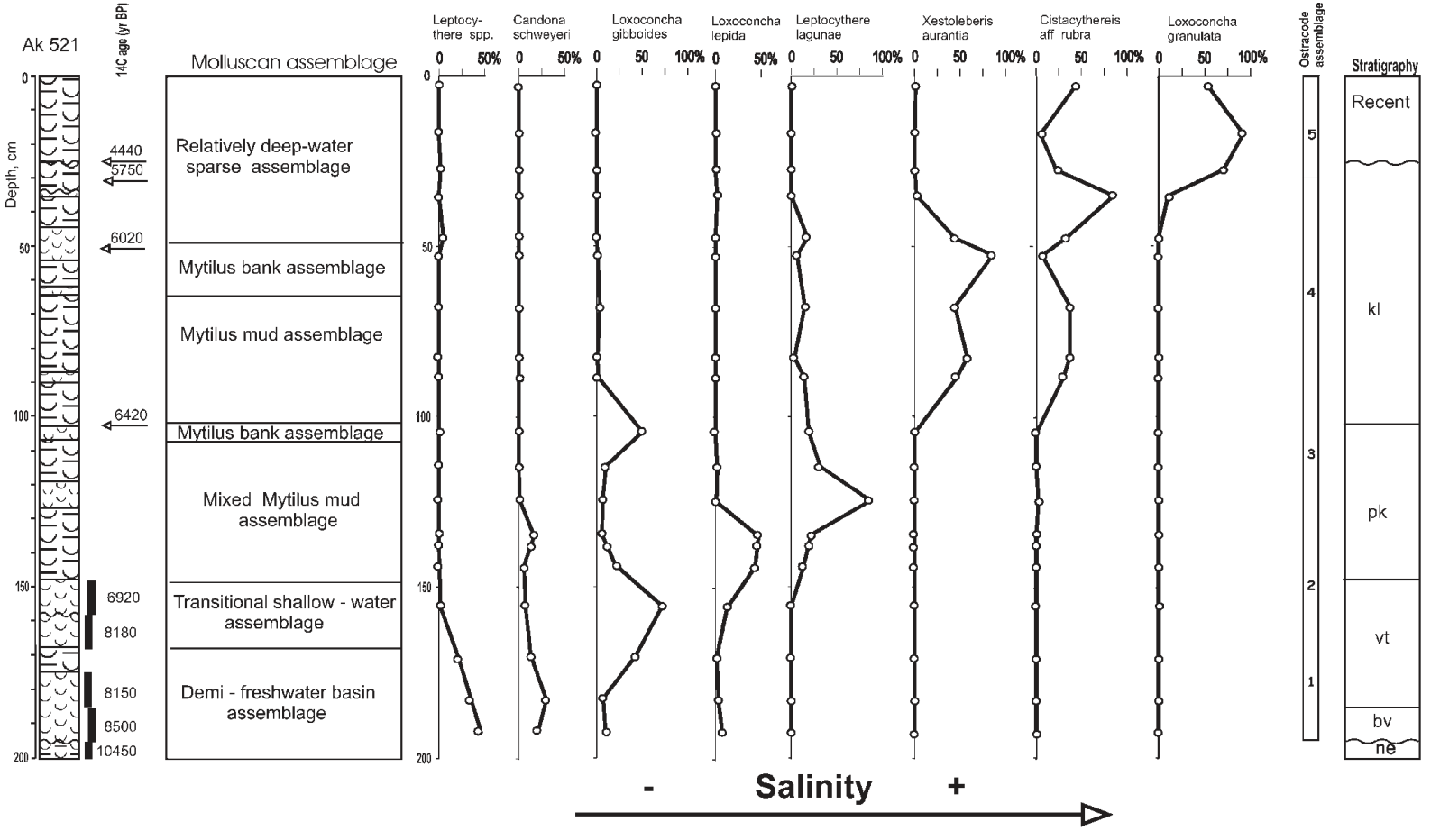

Fig. 10. Lithology, ^{14}C dates, molluscan and ostracode assemblages, and stratigraphic units in core Ak 521 (see Fig. 5 for lithologic symbols). Ostracode species are ranged according to their salinity preferences; the arrow indicates increasing bottom-water salinity.

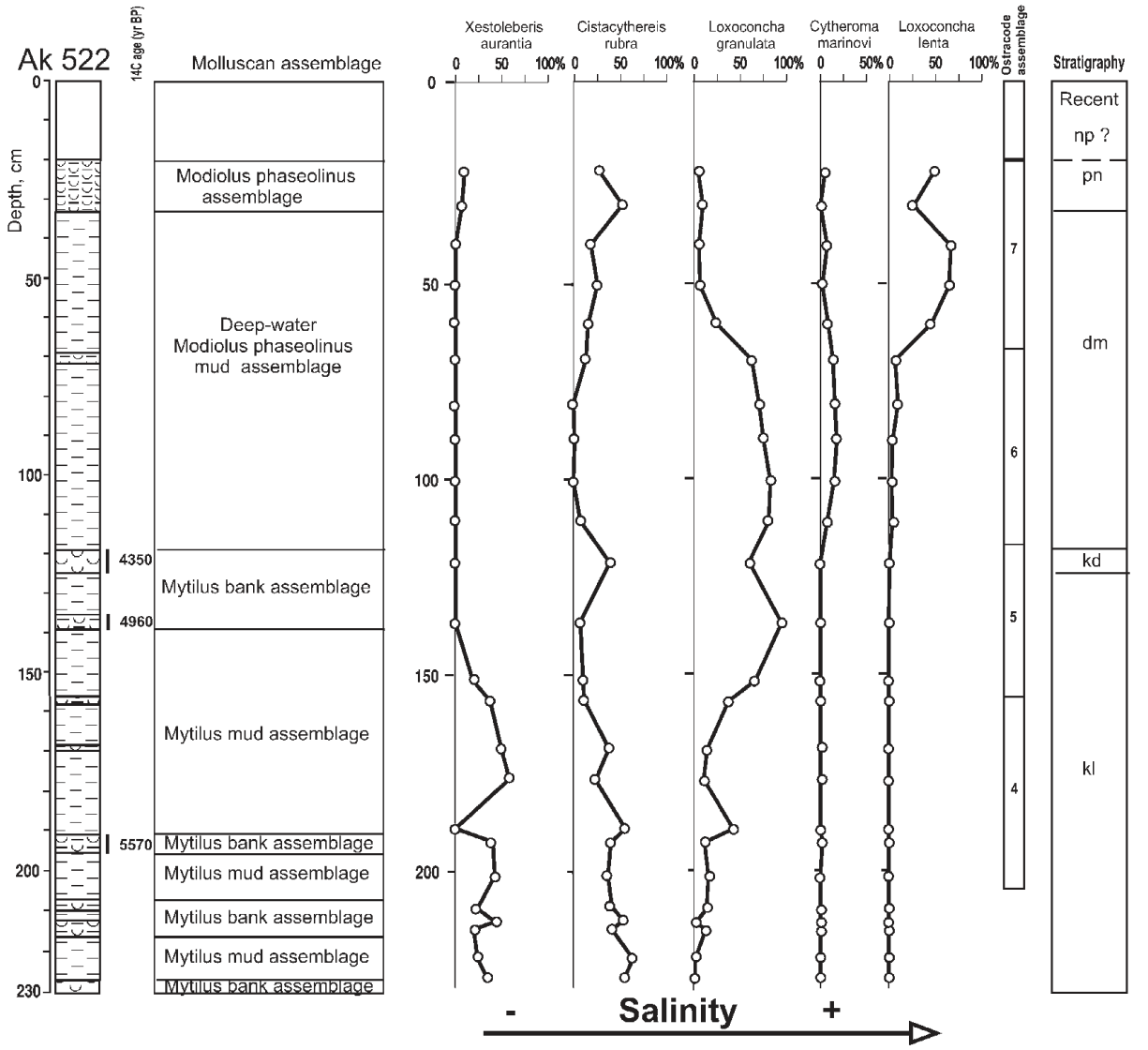

Fig. 11. Lithology, ^{14}C dates, molluscan and ostracode assemblages, and stratigraphic units in core Ak 522 (see Fig. 5 for lithologic symbols). Ostracode species are ranged according to their salinity preferences; the arrow indicates increasing bottom-water salinity.

of *M. edulis*, *M. adriaticus*, and *B. reticulatum* in core Ak 521, and also *C. exiguum*, *Paphia rugata*, *Spicula subtruncata* and juveniles of some other species in cores Ak 500 and Ak 497, suggesting harsh environments with slow to moderate bottom currents and low oxygen content that hindered the ability of mollusks to reach maturity.

3.2.2. Ostracodes

Ostracode assemblages were studied in cores Ak 521, Ak 500, and Ak 522 (Appendix, Tables A5–A7). Species and generic identifications were made by comparisons to photographs and faunal descriptions in the available taxonomic literature, most of which included papers on faunas from the Mediterranean and Black Seas (Livental, 1929; Shornikov, 1969; Colalongo and Pasini, 1980; Kiliç, 2001). The taxonomy of many species of Black Sea ostracodes, especially of diverse genus *Leptocythere*, is in need of revision. Environmental inferences were based on the modern distribution of each species, most notably from its tolerance of various salinity regimes. Even in the case where the species identification was uncertain, many of the identified genera have distinct salinity preferences ranging from fully marine to fresh water conditions

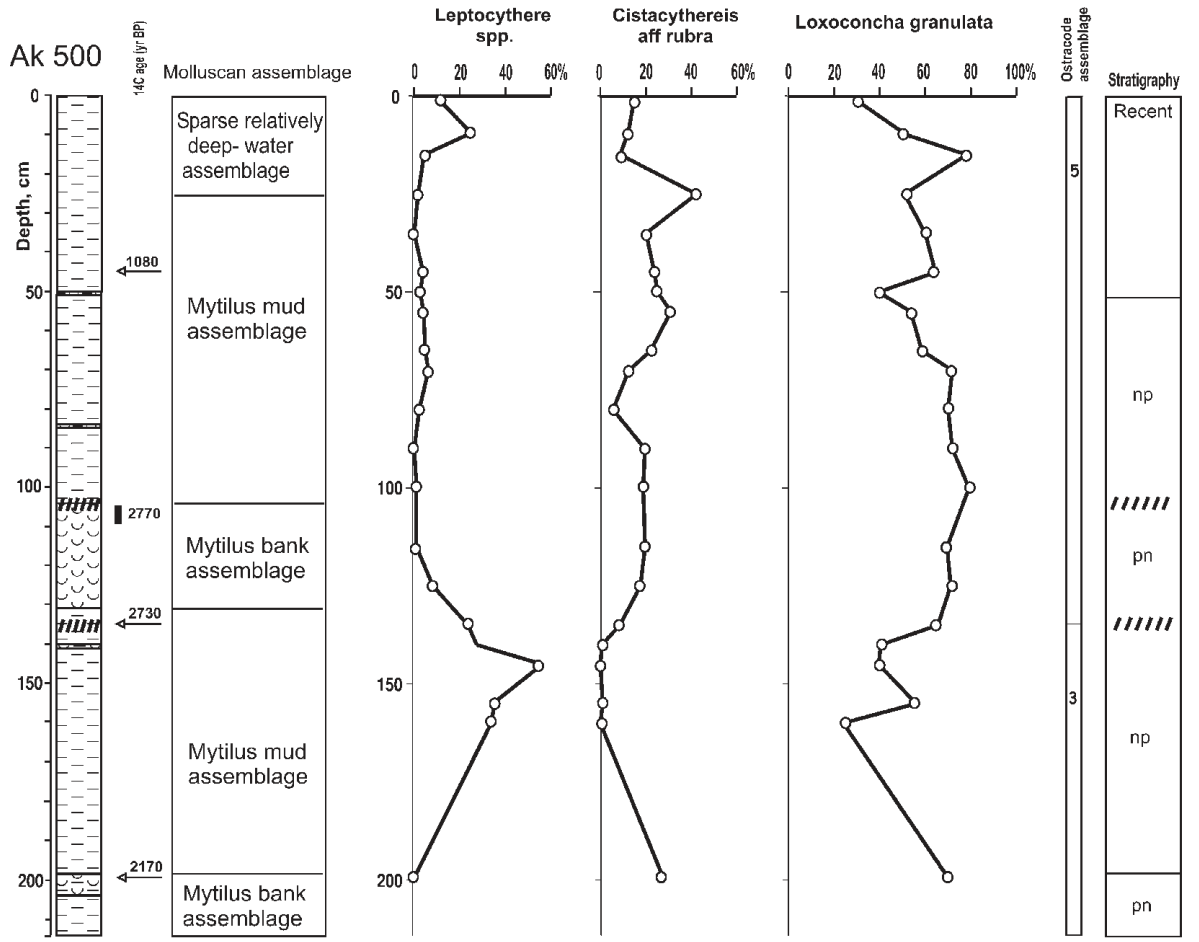

Fig. 12. Lithology, ^{14}C dates, molluscan and ostracode assemblages, and stratigraphic units in core Ak 500 (see Fig. 5 for lithologic symbols).

(Livental, 1929; Shornikov, 1969, 1972; Yanko and Gramova, 1990). Thus, the general patterns of paleosalinity changes are believed to be reliable and apparent in the succession of ostracode assemblages described below for every core.

Core Ak 521 (Fig. 10) contains a series of five gradational ostracode assemblages. Assemblage 1 (195–158 cm) includes common candonids (most are probably *Caspiolla schweyeri*) and at least four species of *Leptocythere*. *Loxoconcha gibboides* and *Loxoconcha lepida* occur in low numbers in these lowermost sediments but increase dramatically in the 158–128 cm interval where they dominate assemblage 2. Assemblage 3 is characterized by an increase in *Leptocythere* cf. *lagunae*, which reaches a peak abundance at about 125 cm, by which time *Caspiolla* has disappeared. Between 120 and 90 cm, *Leptocythere lagunae* decreases and *Xestoleberis aurantia* and *Cistacythereis* aff. *rubra* increase to >50 % and >25 % of assemblage 4, respectively. The uppermost interval of the core (32–0 cm) is dominated by *Loxoconcha granulata* with low numbers of *Cistacythereis* aff. *rubra* and represents assemblage 5.

The ostracode assemblages in core Ak 522 (Fig. 11) demonstrate a pronounced change in the Kundukian shell layer. Whereas assemblage 4 (229–158 cm, Early Kalamitian) contains 3 to 6 species and is dominated by *Cistacythereis rubra* and *X. aurantia*, *L. granulata* becomes the most abundant species upward in assemblage 5 (158–119 cm, Late Kalamitian to Kundukian), and especially in deep-water assemblage 6 (119–66 cm, Early Djemetean). Marine species *Cytheroma marinovi* and *Paradoxostoma variabile* appear in assemblage 6, above the Kundukian layer, whereas oligohaline candonids and some other rare species disappear, suggesting an increase in salinity up to 18–20 psu. Assemblage 7 (66–20 cm,

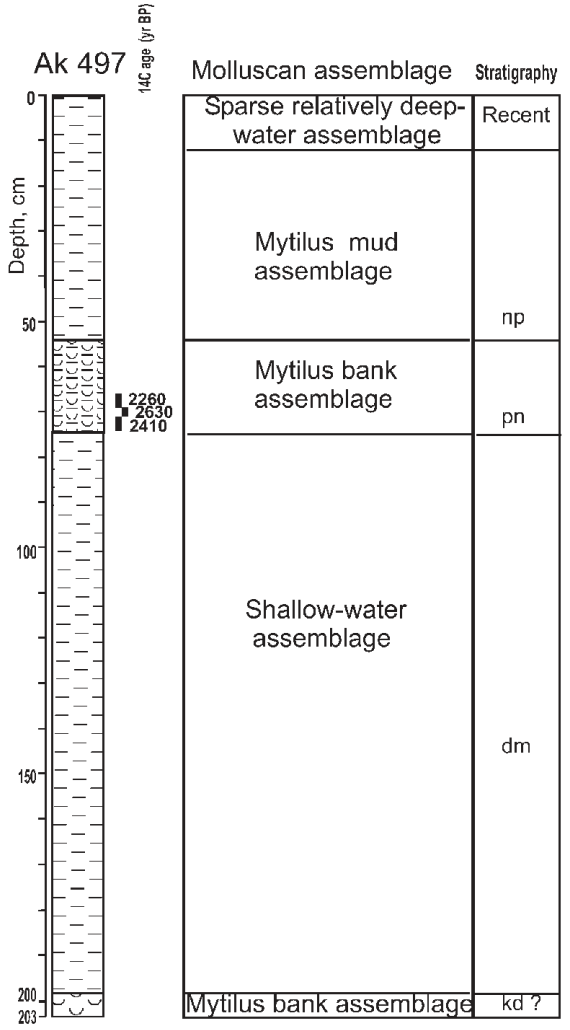

Fig. 13. Lithology, ^{14}C dates, molluscan assemblages, and stratigraphic units in core Ak 497 (see Fig. 5 for lithologic symbols).

Late Djemetean–Phanagorian) is distinguished by the dominance of *Loxoconcha lenta* (a species with an unknown salinity preference) in all samples, except for one interval (33–30 cm) where *C. rubra* is more abundant.

Core Ak 500 (Fig. 12) contains Late Holocene assemblages dominated by *L. granulata* with common *Cistacythereis* aff. *rubra* in the upper 135 cm of the core. This interval appears to correlate with the upper 35 cm of core AK 521. Below the reworked Phanagorean layer, around 155–140 cm, there are significant abundances of several species of *Leptocythere*.

A dominance of candonids and *Leptocythere* in the lower part of Ak 521 points to a narrow annual range of low salinity at 8500–8200 ^{14}C yr BP as candonids thrive in fresh to oligohaline environments (0–5 psu), whereas many *Leptocythere* are known to be oligohaline species. *L. gibboides* and *L. lepida*, abundant at ~150–130 cm in core Ak 521, are considered to be oligohaline rather than freshwater species, according to Yanko and Gramova (1990).

Loxoconcha litoralis, a species found at 113 cm in core Ak 521, is probably mesohaline based on its occurrence in the Mediterranean. *X. aurantia* lives in a wide range of salinities on the Caucasus shelf (Shornikov, 1972; Yanko and Gramova, 1990). The co-occurrence of other ostracode species in the interval dominated by *X. aurantia* at 100–40 cm suggests mesohaline salinity (5–18 psu) and probably a phytal benthic habitat. Oligohaline species are not common in this interval. *X. aurantia* is also abundant in the lower part of core Ak 522 together with *C. rubra,* the latter species seems to prefer slightly more saline environment.

Cistacythereis (referred to as *Hiltermannicythere* or *Carinocythereis* by some authors) is typically found throughout the core Ak 522, and in the upper parts of cores Ak 521 and Ak 500. The genus is thought to be an indicator of polyhaline (18–30 psu) or perhaps slightly less saline ("Stricteurihaline" 11–26 psu of Yanko and Gramova, 1990) environments.

The uppermost part of core Ak 521, from 20 to 0 cm, is characterized by the presence of polyhaline *L. granulata*, together with *Cistacythereis* (18–30 psu) and the marine genus *Bythocythere* (up to 3.8%). *L. granulata* also dominates in the middle part of core Ak 522.

3.2.3. Foraminifers

Benthic foraminifers are not common in the cores and thus they were studied in detail only in Core Ak 521 (Pasechnik, 2003). Thirty-four poorly preserved probably reworked specimens of planktic foraminifers were found only at a few levels. Benthic foraminifers were identified and counted in 56 samples (from 64 sieved samples) and are represented by 12 genera and 25 species and morphotypes (Appendix, Table A8), following the taxonomy of Yanko (1989). The depth and salinity preference of different species are given in the Appendix (Tables A8 and A9).

The lowermost part of the core is barren of foraminifers (Fig. 14). Rare tests, mainly of *Ammonia tepida,* appear at 163 cm and are present up to 87 cm. In the monospecific assemblage 1 (163–140 cm) the species is accompanied only by sparse tests of *Nonion pauciloculum* and *Cribroelphidium percursum.* In assemblage 2 (140–86 cm) *Ammonia compacta*,

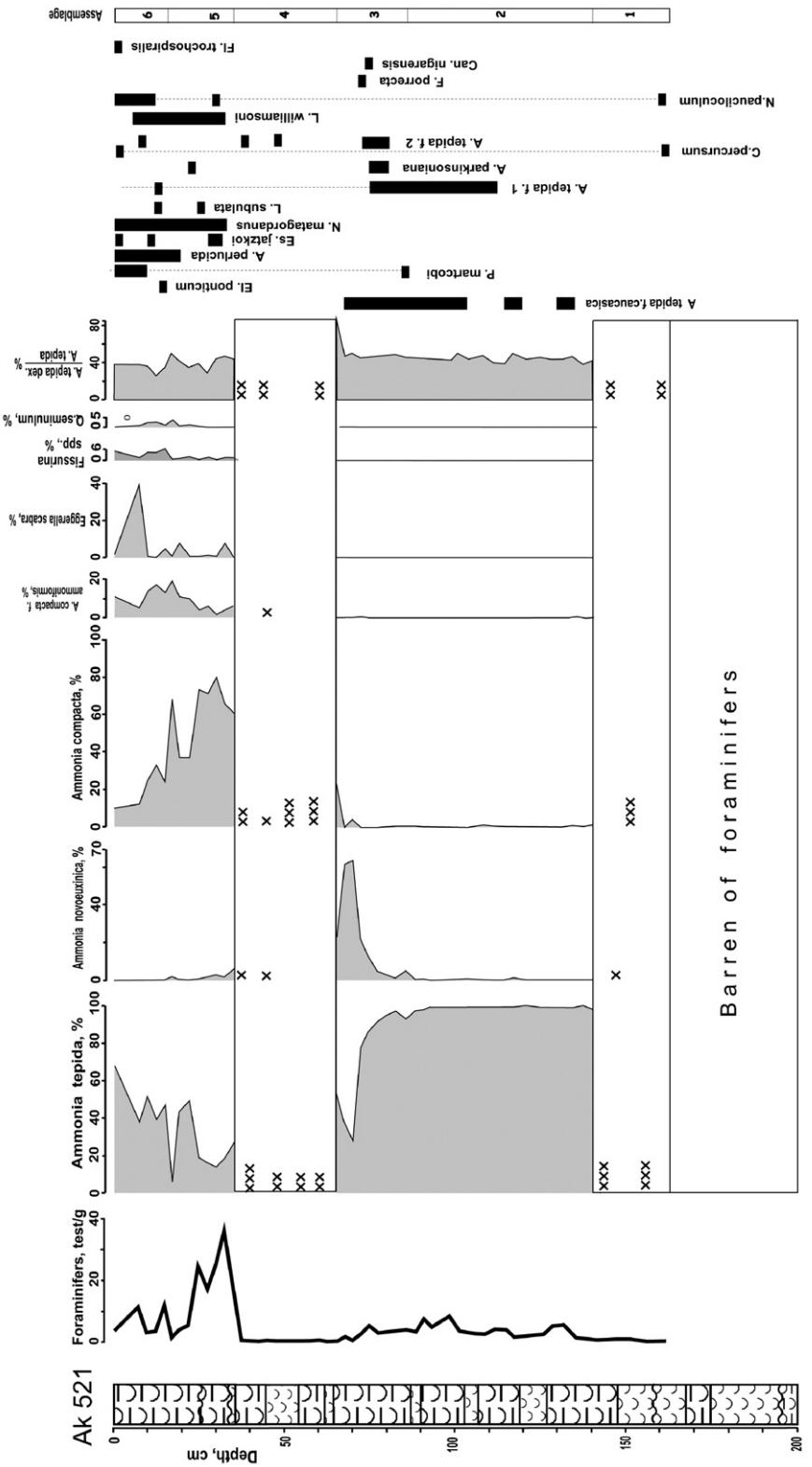

Fig. 14. Benthic foraminifer distribution in core Ak 521 (see Fig. 5 for lithologic symbols).

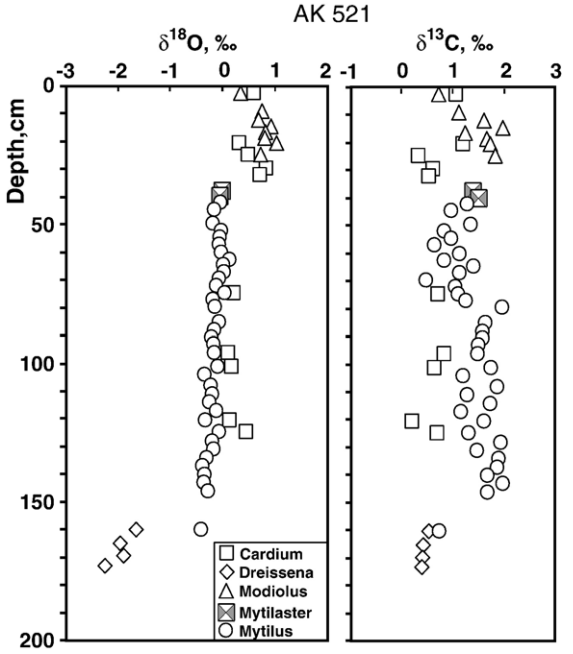

Fig. 15. Average values of oxygen and carbon isotope measurements of monospecific clusters in core Ak 521. *Cardium* = *C. exiguum*, *Dreissena* = *D. rostriformis*, *Modiolus* = *M. phaseolinus*, *Mytilaster* = *M. lineatus*, *Mytilus* = *M. edulis*.

A. novoeuxinica, *A. tepida* forma *caucasica*, and *A. compacta* forma *ammoniformis* occur together. Large adult benthic foraminifers are especially abundant at 133–130 cm, whereas small tests common in the shelly layer (110–107 cm) indicate harsh environments.

Assemblage 3 (86–65 cm) is diverse and dominated by *A. tepida* and *A. novoeuxinica*, locally accompanied by *A. compacta*, *A. tepida* forma *caucasica*, *A. tepida* forma 1 and 2, *A. compacta* forma *ammoniformis*, *A. parkinsoniana, Porosononion martcobi ponticus*, and *Fissurina porrecta* at different levels. Assemblage 4 (65–34 cm) is very sparse.

Between 34 and 16 cm, *A. compacta* and *A. tepida* dominate diverse assemblage 5 with several accessory species such as *Eggerella scabra*, *A. tepida* forma *ammoniformis*, *Laryngosigma williamsoni*, and *Nonion matagordanus* also present.

The dominance of *A. tepida*, the upwardly decreasing abundance of *A. compacta*, and the moderate abundance of *A. compacta* forma *ammoniformis* is characteristic of assemblage 6 (16–0 cm). *Quinqueloculina seminulum*, *Fissurina spp.* group, *N. pauciloculum*, *Esosyrinx jatzkoi*, *Laryngosigm subulata* and planktic foraminifers persist in small amounts, whereas several other species appear sporadically. The fragile agglutinated species *E. scabra* (at 9–6 cm) suggests a brief interval of low-energy environment. *P. martcobi ponticus*, *A. tepida* forma *caucasica* and *A. tepida* forma 2 occur intermittently in this interval.

The pattern of foraminiferal assemblages and the paleoecological data on different species (Appendix, Tables A8 and A9) indicates that assemblages 1–3 (~8200–6100 ^{14}C yr BP) were deposited in relatively shallow-water environments, with bottom salinity ranging from 5 to 18 psu. These assemblages are dominated by shallow, cold-water mesohaline species, and contain few polyhaline species. In the Late Holocene deep-water polyhaline and relatively warm-water species become more abundant and even dominate assemblage 5.

3.3. Oxygen and carbon isotopes

In core Ak 521 (Fig. 15; Appendix, Table A10), the δ^{18}O of the fresh-water mollusk *Dreissena rostriformis* shows an increase from very negative values in the lowermost part of the core (from the end of the Neo-euxinian to the Vityazevian), whereas the δ^{18}O of *Mytilus edulis* shows a slight enrichment from 163 to 40 cm during the Vityazevian–Kalamitian transgression

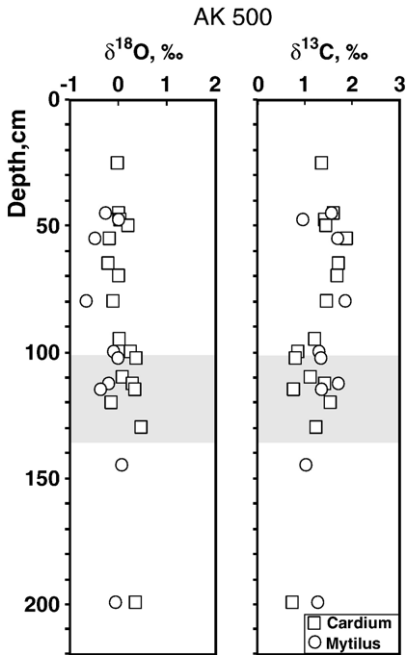

Fig. 16. Average values of oxygen and carbon isotope measurements of monospecific clusters in core Ak 500. *Cardium* = *C. exiguum*, *Mytilus* = *M. edulis*. The reworked Phanagorean layer is marked in grey.

overprinted by variations on the order of 0.2–0.3‰ (2–3 times greater than the average standard deviation of measurements of monospecific clusters noted in Section 2.2.3) approximately every 20 cm. The $\delta^{18}O$ record of *M. edulis* is supported by a few measurements on *Mytilaster lineatus* and by several analyses of shells of *Cardium exiguum* collected from the same horizons as the *Mytilus* samples. The most positive values, 0.3–1‰, were obtained on *C. exiguum* and *M. phaseolinus* from the upper part of the core, above 34 cm.

The $\delta^{13}C$ of *D. rostriformis* below 158 cm is very uniform, whereas that for *M. edulis* demonstrates a sharp initial increase from 0.7‰ at 158 cm to 1.7‰ at 148 cm, remains within the range 1–2‰ up to 70 cm, and then decreases to fairly uniformly slightly lower values in the interval 70–40 cm. A general depletion trend is found in the $\delta^{13}C$ of *M. phaseolinus* in the uppermost 34 cm of the core.

The pronounced variability of $\delta^{18}O$ and $\delta^{13}C$ records in the middle part of core Ak 500 (Fig. 16; Appendix, Table A11) may be related to the reworked Phanagorean sediments between 136 and 104 cm; the values at 104 cm are nearly identical to those at 200 cm for both *C. exiguum* and *M. edulis*. In the upper part of the core, the $\delta^{18}O$ value of *C. exiguum* exhibits about half of the variability of that of *M. edulis*. The $\delta^{13}C$ variations shown by both species in the same upper part of the core do not exceed 0.5‰, if one sample of *M. edulis* at 47.5 cm is not included.

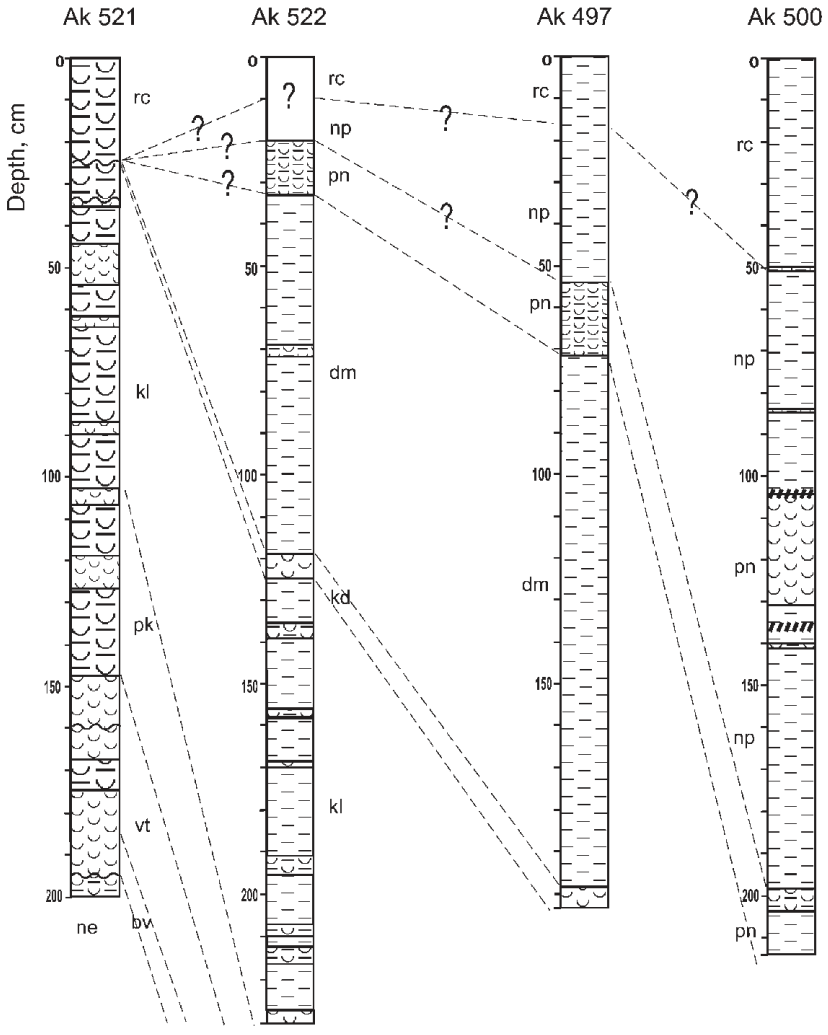

Fig. 17. Correlation of sediment cores (see Fig. 5 for lithologic symbols).

4. Discussion

Seismic, sedimentological, faunal, stable isotope data and ^{14}C dates allow stratigraphic units distinguished in the four cores to be correlated with high and low Black Sea level stands (Figs. 4 and 17). We reconstructed the main features of Caucasian shelf paleoenvironments specific for five transgressive–regressive cycles superimposed on glacioeustatic sea-level rise. Along with the rise in sea level, there is a corresponding increase in salinity during the Holocene due to a progressively enhanced estuarine circulation and saline bottom water inflow from the Mediterranean. The three younger cycles are much better represented in our material compared to the two older cycles due to extensive erosion of Neoeuxinian to Vityazevian sediments at the shelf edge. It's noteworthy that sea-level low stands are represented by widely extensive shell layers and seismic reflectors during the most pronounced regressions.

4.1. Neoeuxinian–Bugazian cycle (~10,500–8200 ^{14}C yr BP)

Seismic data interpreted by extrapolation of the Ak-521 record suggest that the Caucasian outer shelf was flooded at about 11,000–12,000 ^{14}C yr BP by waters of the Neoeuxinian semi-freshwater basin (i.e. demi-freshwater basin by Nevesskaya (1965) and Chepalyga (2002)), which occupied the outer shelf up to about 50 m below the present sea level at the transgression maximum. Thus, according to our ^{14}C data, the oldest sediments recovered in core Ak 521 only (Figs. 10 and 17) represent the final stage of this basin with relative sea level about 20 m below present (Balabanov and Izmailov, 1988; Chepalyga, 2002). This stage was terminated by the Neoeuxinian–Bugazian regression about 10,000–9000 ^{14}C yr BP (Fig. 4). The presence of four mollusk species which migrated from the Caspian Sea, and the absence of the mollusk *Didacna* and foraminifers, suggest a low salinity of about 5 to 8 psu and low annual variability. Similar salinity values were previously suggested for the Late Neoeuxinian by Nevesskaya (1965) and Degens and Ross (1972). The regular occurrence of *D. rostriformis* suggests sluggish bottom currents and low levels of dissolved oxygen. Stable stratification and poor ventilation resulted from the input of low-salinity Black Sea water, at the same time similar water occupied the Marmara Sea (Aksu et al., 2002). Caspian mollusks penetrated into the Black Sea via the Manych Strait for the final time during the Early Khvalynean transgression, 16,000–14,000 ^{14}C yr BP (Chepalyga, 2002). Many authors have argued that the Neoeuxinian basin had unidirectional flow into the Marmara Sea via the Bosphorus at ~10,000–9000 ^{14}C yr BP (Fedorov, 1978; Aksu et al., 2002; Mudie et al., 2002; Hiscott et al., 2002; Kaplin and Selivanov, 2004). However, the assumption that this flow existed until 7200–6500 ^{14}C yr BP (Görür et al., 2001; Algan et al., 2001) is not supported by our data.

Our ^{14}C dates suggest there was an ~1000-year-long hiatus about 10,000–9000 yr BP correlating with the seismic reflector *A* (Figs. 5 and 10), as sea level reached its minimum stand prior to the Bugazian transgression (Fig. 4). The presence of Caspian mollusks and oligohaline ostracodes dominated by *Leptocythere* spp. and *Caspiolla schweyeri* up to 158 cm in core Ak 521 indicate that a semi-freshwater environment likely existed on the Caucasian shelf until the Early Vityazevian transgression. The low $\delta^{18}O$ values of *D. rostriformis* from this interval are more typical of low-salinity than marine waters (Major et al., 2002). However, these $\delta^{18}O$ values are higher than those measured on the same species in the northwestern Black Sea during deglaciation when the supply of fresh water was greater (Bahr et al., 2005).

The condensed shell-rich section recovered in the lower 50 cm of core Ak 521, with its low sedimentation rates (Figs. 9 and 10), hiatuses, erosion and sediment reworking events (as indicated by a slight age inversion, Table 2) represents a typical, relatively shallow-water, high-energy shelf-edge facies. This environment existed at the shelf edge up to at least 6900 ^{14}C yr BP, thus including a major part of the Vityazevian transgression (Fig. 4).

The lower boundary of the *Vityazevian–Prekalamitian cycle* (~8200–6400 ^{14}C yr BP) is distinguished by the first appearance of shallow-water marine fauna (*C. exiguum*, *M. edulis*, *O. edulis*) on the Caucasian shelf (at 168 cm in core Ak 521, Fig. 10). By this time, the Black Sea level was about 10 m below present (Balabanov and Izmailov, 1988; Chepalyga, 2002; Fig. 4). The first appearance of benthic foraminifers is established at 163 cm. Caspian mollusks co-existed with marine mollusks during the Vityazevian transgression, which is represented mainly in core Ak 521 by a shell layer deposited during a short low sea-level stand. *D. rostriformis* appears to have survived through at least a portion of the Prekalamitian regression (Appendix, Table A1). Therefore, this cycle is

characterized by mixed molluscan assemblages that reflect a progressive transition from semi-freshwater to semi-marine environments (Nevesskaya, 1965; Chepalyga, 2002). This finding does not support the hypothesis by Ryan et al. (1997, 2003) for a catastrophic flooding of the Black Sea by Mediterranean waters. Our conclusion is consistent with recent estimates (Myers et al., 2003) of the minimal time necessary for the salinification of the basin up to semi-marine values. The date of ~8200 ^{14}C yr BP is very close to the date of brackish fauna appearance on the mid-shelf in the western Black Sea at 8400 ^{14}C yr BP (Major et al., 2002).

The Vityazevian cycle terminates with the Prekalamitian low sea-level stand followed by a major transgressive phase. The condensed shelf-edge facies was replaced by a rapidly accumulating shelly mud facies at Ak-521 reflecting intense terrigenous supply, slow bottom currents, and moderate to poor bottom water ventilation. High proportions of juveniles in molluscan assemblages point to unfavorable environment.

Although the deep part of the sea was already filled with Mediterranean waters by the Early Vityazevian time (Ostrovskii et al., 1977), the salinity of the upper waters on the shelf probably remained as low as 10 psu (Nevesskaya, 1965). This inference is consistent with the paucity of benthic foraminifera and the strong dominance of oligohaline ostracode species. An increase in bottom water salinity is inferred from the disappearance of Caspian mollusks and from progressively heavier δ^{18}O values of *D. rostriformis* during the Vityazevian transgression (Fig. 15). Although there appears to be a pronounced shift in δ^{13}C values of *M. edulis* between 160 to 146 cm (Fig. 15), it is not clear whether this shift indicates a significant change in hydrological regime and river discharge at the transition from the Vityazevian transgression to the Prekalamitian regression or whether variations in other parameters such as the δ^{13}C of dissolved inorganic carbon (DIC) and dissolved organic carbon (DOC), DIC/DOC, amount of solar radiation, or possible vital effects (Vander Putten et al., 2000; Elliot et al., 2003; Surge and Walker, 2006), are responsible for the shift in the δ^{13}C of *M. edulis*. The apparent magnitude of the shift may also be enhanced by the unusually large difference between the measured δ^{13}C values (0.066 and 1.389‰) of the two *M. edulis* shells from 160.5 cm that were averaged before plotting on Fig. 15. In contrast, the δ^{18}O values of individual shells within clusters of *D. rostriformis* and *M. edulis* at 160 cm, and of individual shells of *M. edulis* at 146 cm, are clustered quite tightly. Unlike many other carbonate-secreting organisms, mollusks tend to deposit their shells nearly in oxygen isotopic equilibrium with ambient waters (see review in Sharp, 2006). Although the consistent positive offset of 0.2–0.4‰ between *C. exiguum* and *M. edulis* between 125 and 75 cm may be due to vital effects, it seems unlikely that the difference of over 1.2 ‰ between the δ^{18}O values of *D. rostriformis* and *M. edulis* at 160.5 cm is related wholly to this phenomenon. Since the shells from the horizon centered at 160.5 cm were actually sampled from a 5-cm-thick sediment layer between 158 and 163 cm that took over 600 yr to accumulate (Fig. 9), they may not be exactly coeval, further complicating the evaluation of potential vital effects.

4.2. Kalamitian–Kundukian cycle (~6400–4100 ^{14}C yr BP)

Sea level reached its modern value at ~6000 ^{14}C yr BP, during the Kalamitian transgression (Fig. 4; Chepalyga, 2002). Several authors believe that it may have reached ~2 m above the present level (Fedorov, 1985; Balabanov and Izmailov, 1988; Kaplin and Selivanov, 2004). The Kalamitian transgression and the following Kundukian regression (about — 22 m below present, according to Chepalyga (2002)) are represented in core Ak 521 and especially core Ak 522 (Fig. 17). The strong reflector B in the upper part of the Kalamitian unit is related to a hiatus, expressed as a sharp decrease in linear sedimentation rates (from 70–128 cm/ka to ~6 cm/ka, Fig. 9). Reflector C is expressed in core Ak 522 as a Kundukian-dated shell layer and in core Ak 497 as the bottom shell layer corresponding to the Kundukian regression (Figs. 2, 3 and 13). The sediments of this cycle include alternating mud and shell layers, the shells being more abundant in core Ak 521 from the shelf edge than in core Ak 522 from the outer shelf. In the latter core, the cycle ended with the Kundukian regression, marked by a distinct transition from Kalamitian "mytilus mud" below to Djemetean "phaseolina mud" above, at 4350±100 yr BP (Fig. 11).

Molluscan assemblages are generally characterized by a low diversity and strongly dominated by *M. edulis* likely due to very high sedimentation rates, which inhibited other species. A conspicuous number of juveniles supports unfavorable ecological conditions. Ostracode and foraminifer assemblages differ

considerably from the older ones. Polyhaline species *C. rubra* and *X. aurantia*, which tolerate a wide range of salinity, dominate among ostracodes whereas oligohaline species occur very rarely (Figs. 10 and 11; Appendix, Tables A5 and A6). Although foraminifer assemblages became more diverse, shell layers are generally characterized by a low abundance of tests (Fig. 14). The highest abundance and very diverse assemblages dominated by warm-water polyhaline *A. compacta* occur at the end of the transgression. All faunal data support an increase in bottom water salinity to ~15–18 psu, thus promoting a proliferation of diverse marine assemblages. In general, faunal assemblages during the transgression suggest lower hydrodynamics and oxygen content compared to regressive phases, which are characterized by strong bottom currents and well-ventilated environments.

The main part of the Kalamitian transgression is characterized by constant oxygen isotope values of *M. edulis* and *C. exiguum* (Fig. 15; Appendix, Table A10), with a slight upward enrichment, which confirms an increase in bottom-water salinity. The low-amplitude variability (up to 0.2–0.3 ‰) of $\delta^{18}O$ measured on *M. edulis* nearly every 20 cm suggests a higher-frequency cyclicity of approximately 200 yr duration (Fig. 9) likely due to repeated variations in precipitation and evaporation. Lamy et al. (2006) have distinguished 800-year and 500-year cycles in clay layer frequency in sediment cores from the southwestern Black Sea extending 7500 cal yr BP. They relate the patterns of these multicentennial variations to the Arctic Oscillation/North Atlantic Oscillation (AO/NAO), which, when in its negative phase, enhances rainfall in this region, resulting in intervals of higher clay layer frequencies. Although the $\delta^{18}O$ cycles described above in *M. edulis* are of higher frequency than the predominant clay layer cycles, there is a pattern of higher-frequency, lower-amplitude clay layer cyclicity between 7000 and 6000 cal yr BP, suggesting that the cyclicity in $\delta^{18}O$ may also have been influenced by the AO/NAO during the main Kalamitian transgression. Conversely, $\delta^{13}C$ varied considerably during the same Kalamitian interval, which might be related to possible variations in the parameters that affect $\delta^{13}C$ as described above for the Prekalamitian regression. Oxygen isotope data (especially on *C. exiguum*) suggest a pronounced change in paleoenvironment around the time of the hiatus at ~5700 ^{14}C yr BP, in line with a marked decrease in sedimentation rate (Fig. 9).

The boundary between Kalamitian and Djemetean high stands, i.e., the Kundukian regression, is well represented and dated in core Ak 522 (Fig. 11). The *Djemetean–Phanagorean cycle* is characterized by different types of sediments (Fig. 17) and benthic thanatocoenoses in the cores from the SE and NW profiles due to a difference in water depth. In core Ak 522 this cycle is represented by a rather deep-water phaseolina mud accumulated during the Djemetean transgression and by a shell layer enriched in *M. phaseolinus* which most probably corresponds to Phanagorean regression, when the level of the Black Sea was about 13 m below present (Arslanov et al., 1982; Chepalyga, 2002; Fig. 4). Marine ostracode species *Cytheroma marinovi* and *Paradoxostoma variabile* appear in Early Djemetean assemblages, which are strongly dominated by polyhaline species *L. granulata* (Fig. 11). Rather diverse mollusk and ostracode assemblages point to high salinity (likely about 18–20 psu), low temperature, relatively low-energy bottom environment with restricted ventilation during the high stand at water depth ~90 m. A pronounced increase in the abundance of *M. phaseolinus* in the Phanagorean layer suggests rather active hydrodynamics, moderate oxygen content and low bottom-water temperatures. The latter was likely maintained by a shallow thermocline. Unfortunately, this cycle cannot be distinguished in the upper part of core Ak 521 due to extremely slow sedimentation or even local erosion. Therefore, it is impossible to characterize foraminiferal assemblages studied only in this core.

The Djemetean silty muds in core Ak 497 contains shallow-water mollusk assemblages with *C. exiguum*, *Cerithium vulgatum* and a few shells of some other species (Fig. 13) developed in a relatively unfavorable environment. On the contrary, the Phanagorean shell layer in cores Ak 497 and Ak 500 is characterized by a highly diverse *Mytilus* bank assemblage containing 11 to 13 mollusk species, thus pointing to intense mixing and ventilation at very shallow depth (about 30–45 m). At some levels *C. paucicostatum* becomes the most abundant species.

According to our ^{14}C dates (Tables 1 and 2, Fig. 12), Phanagorean sediments are found below and within the younger Nymphaean layer in core Ak 500. In the latter case, they are most likely reworked due to slumping from the shelf edge. This is supported by the ^{14}C-date inversion and a change in molluscan assemblages at this boundary (101–136 cm), as well as by the angular unconformity noted in both the core description and the seismic record. Variable

$\delta^{18}O$ and $\delta^{13}C$ values on within the layer (101–136 cm), and similar isotopic compositions at 101 and 200 cm, the top of both the reworked and *in situ* Phanagorean layers (Fig. 16, Appendix, Tables A3 and A11), respectively, also provide strong evidence of reworking. The Phanagorean regression (low stand) is dated archeologically at 2700–2300 cal yr BP (Chepalyga, 2002) and at 2630±160 ^{14}C yr BP (Ostrovskii et al., 1977). These dates are surprisingly close to each other by absolute value (i.e., without calibration of the ^{14}C date) which points to uncertainty in the age of the Phanagorean unit as a whole. However, we consider the upper shell layer in core Ak 497 with a slight inversion of one of three dates (Table 2, Fig. 13), and the lower shell layer in core Ak 500 (dated at 2170±40 ^{14}C yr BP), to be related to this low-stand event. This interpretation is consistent with our seismic data, which show that the positions of the indistinct reflector D at station Ak 497 (Fig. 8) and the reflectors D and D_1 at station Ak 500 (Fig. 7) correspond to both ^{14}C-dated shell layers.

The youngest *Nymphaean* to *Recent cycle* is better represented at the NW shallow-water profile off Gelendjik than at the SE profile. However, we could date only one horizon in core Ak 500, which roughly corresponds to the beginning of the Little Ice Age (1080±45 ^{14}C yr BP or 660–520 cal yr BP, Fig. 12; Murdmaa et al., 2004; Matthews and Briffa, 2005). In general, the diversity and abundance of mollusk species decrease during this cycle in cores Ak 500 and Ak 497 (Appendix, Tables A3 and A4). A diverse *Mytilus* mud assemblage in the lower part of Nymphaean layer is replaced upward by a deep-water one. A similar sparse assemblage likely of the same age is also found at the top of core Ak 521 (Fig. 10). Conversely, the foraminiferal assemblage is rather diverse (Fig. 14) and represented by deep-water polyhaline and relatively warm-water species. Moderate to low hydrodynamics and restricted ventilation may be suggested as a whole for this cycle. Polyhaline *L. granulata* and *Cistacythereis* aff. *rubra* dominate the ostracode assemblages during the cycle, consistent with modern salinity of about 20 psu. In this context it is difficult to explain the surprisingly high abundance of oligohaline *Leptocythere* spp. during the Early Nymphaean in core Ak 500 (Fig. 12).

The few $\delta^{18}O$ and $\delta^{13}C$ measurements on from this cycle in core Ak 500 (Fig. 16) show moderate variability, up to 0.7 and 1.0‰ respectively, likely due to variations in evaporation, precipitation and river discharge.

5. Conclusions

1. Paleontological, paleoecological, sedimentological, geochemical and seismostratigraphic data, and ^{14}C age dates, obtained from the Eastern (Caucasian) shelf, demonstrate pronounced differences in paleoenvironments which characterized high and low sea-level stands during five transgressive–regressive cycles overprinted on the glacioeustatic Black Sea level rise and increase in bottom water salinity during the last 11,000 yr.
2. The first appearance of Mediterranean mollusks on the outer Caucasian shelf is dated at ~8200 ^{14}C yr BP, being followed somewhat later by the appearance of benthic foraminifers, whereas the transitional mollusk assemblages existed there until ~6900–6500 ^{14}C yr BP.
3. Faunal assemblages on the outer shelf were strongly influenced by sea-level changes and differed from each other when inhabiting various water depths within the same stratigraphic unit or time interval.
4. Transgressions and sea-level high stands are generally characterized by slow to moderate hydrodynamics and restricted ventilation, whereas strong currents and high bottom-water oxygen content are typical for low-stand environments, particularly during the Phanagorian and Kundukian regressions.
5. High-energy bottom environments favored the formation of shell layers, while low-energy conditions favored rapidly accumulating mud layers. The high-energy shell facies, formed due to the removal of mud by bottom currents, commonly mark low sea-level stands, whereas mud or shelly mud facies are deposited during transgressive phases characterized by relatively low bottom-water hydrodynamic activity. Most prominent shell layers and hiatuses correlate with seismic reflectors, thus providing evidence for correlation of core sections and paleoenvironmental events.

Acknowledgements

We thank the captain, crew and participants of cruise 27 by the RV *Akvanavt*. We are also thankful to G. N. Alekhina for drawing figures, T. N. Alekseeva for assistance in the cleaning mollusk shells before age dating, NOSAMS, Woods Hole Oceanographic Institution, Beta Analytic and L. D. Sulerjitsky for performing the ^{14}C analyses. We gratefully acknowledge the discussion with E. Bard and L. Vidal which helped to properly estimate conventional ^{14}C ages based on routine ^{14}C dating.

Appendix A

Table A1
Mollusk species distribution in Core Ak 521

Depth, cm	*Mytilus edulis*	*Ostrea edulis*	*Cardium exiguum*	*Cardium edule*	*Modiolus adriaticus*	*Modiolus phaseolinus*	*Modiolus lineatus*	*Modiolus sp*	*Corbula gibba*	*Bittium reticulatum*	*Retusa truncatula*	*Trophon muricatus*	*Hydrobia sp.*	*Dreissena rostriformis*	*Monodacna caspia*	*Theodoxus pallasi*	*Micromelania sp*
6– 9	x				x	x											
26–29	x		x		x	x				x							
34–36	x		x				x										
44–46	x																
46–49	fr				juv												
49–51	fr										x	x					
51–54	A																
62–64	x								x								
81–84	x												x				
87–90	A		x		x								x				
98–100	x		x	x									x				
102–107	A		x		juv						x						
113–116	A												x				
119–123	A		x	x													
127–130	A		x	x	x								x	x			
133–136	A												x	x			
139–142	A				juv									x			
145–148	A							juv									
148–153	x			x									x	x			
153–158	x													x	x		x
158–163	x													x	x		x
163–168	x	x		x					x					x	x		x
168–172														x	x		x
175–180														x			x
183–185														x			x
185–190														x			x
190–195														x			
195–200			x											x		x	x

Appendix B

Table A2
Mollusk species distribution in Core Ak 522

Depth, cm	*Mytilus edulis*	*Mytilus sp*	*Cardium exiguum*	*Cardium sp.*	*Modiolus adriaticus*	*Modiolus sp.*	*M. phaseolinus.*	*Mactra subtruncata*	*M. corallina*	*Corbula gibba*	*Bittium reticulatum*	*Retusa sp.*	*Micromelania sp.*	*Cerastoderma edule*	*Pirenella sp.*	*Nassarius reticulatus*	*Nassarius sp.*	Unidentified bivalve fragments
20–25							A		x		x	x		x				
30–33							A		x									
40–43							A		x		x	x						
50–53							A		x		x							
60–63							A				R	R						
69–72							A				x	x						
80–83			R juv			A												
90–93							A				x	x						
100–103							A + fr								fr juv			
110–113	R				A			x			R	x				R		
119–125	A									juv							juv	
135–139	A	A								x								

150–153	A + fr		R														
156–158	A																
168–170	A + fr																fr
175–179	A													R juv			
188–191	A + fr																
191–195	A		juv						juv			juv					
200–203	A + f																
209–210	A fr																
212–214	A fr																A fr
214–216	A fr																
221–224	A fr																
226–229	A fr									x							A fr

Appendix C

Table A3
Mollusk species distribution in Core Ak 500

Depth, cm	*Mytilus edulis*	*Cardium exiguum*	*C. paucicostatum*	*Modiolus adriaticus*	*Mactra corallina*	*Mactra subtuncata*	*Pitar rudis*	*Paphia rugata*	*Scorbicularia plana*	*Bittium reticulatum*	*Nassarius reticulatum calatus*	*Calliptraea chinensis*	*Retusa truncatula*	*Trophon muricatus*	*Patella sp.*	*Vermetus sp*	Unidentified bivalve fragments
0–2		x							x								
4–6		fr	fr														fr
9–11	fr									x							fr
14–16	fr	fr				juv							juv				
19–21		x		x				x									
24–26		x		x													
34–36	x			x													
49–51	x	x		x													
54–56	x	x		x													
79–81	x	x		x													
101–104	x	x	x	x						x				x		x	
111–114	x	x	x	x						x				x		x	
114–116	x	x		x			x			x							
119–121		x					x			x			x				
124–126	A									x							
129–131	A	x		x						x						x	
134–136		x		x						x	x				x		
139–141		x		x	juv					A		x					
144–146	x			fr	juv					A							
149–151		R	x	fr	A					A							
154–156	x	x			juv					A							
159–161		R		juv	juv												
199–200	x	x	x	x			x			x		x		x		x	

Appendix D

Table A4
Mollusk species distribution in Core Ak 497

Depth, cm	*Mytilus edulis*	*Cardium exiguum*	*C. paucicostatum*	*Modiolus adriaticus*	*Spisula subtruncata*	*Paphia rugata*	*P. discrepans*	*Divaricella divaricata*	*Scorbicularia plana*	*Cerithium vulgatum*	*Bittium reticulatum*	*Nassarius retculatulus*	*Trophon muricatus*	*Patella sp.*	*Vermetus sp.*
0–4		x													
4–6	fr	x			x										
9–11		x		x	x										
14–16	x	x											x		
19–21	x	x													
24–26		x			x										
29–31	x	x		x			x								
34–36	x	x		x		x									
39–41	x	x		x											
44–46		x			x										
54–56	x		A	x	x						x				
64–66	x		A	x							x			x	
74–76	x	x		x	x	x	x	x	x	x			x		
109–111		x			x					x					
134–136										juv					
169–171		x										x			x
174–176										x					
184–186	x								x						

Appendix E

Table A5
Ostracode species distribution in Core Ak 521, %

Depth, cm	*Cistacythereis aff rubra*	*Loxoconcha granulata*	*Loxoconcha gibboides*	*Loxoconcha spiked*	*Loxoconcha lepida*	*Leptocythere aff ramosa*	*Leptocythere cymbula*	*Leptocythere cf rara*	*Leptocythere large, pitted*	*Leptocythere lagunae*	*Leptocythere olivana*	*Callistcythere lobiancoi*
0–6	42.7	53.13	0	0	0	0	0	0	0	0	0	0
16– 18	4.55	91.61	0	0	0	0	0	0	0	0	0	0
26–29	22	70	0	0	0	0	0	0	0	0	2	0
34–36	85.1	10.64	0	0	2.13	0	0	0	0	0	0	0
46–49	32.1	0	0	0	0	0	0	3.57	17.9	17.9	0	0
51–54	6.32	0	1.05	0	0	0	0	0	0	6.32	0	0
66–69	37	0	3.7	0	0	0	0	0	0	14.8	0	0
81–84	36.6	0	0.89	0	0	0	0	0	0	3.57	0	0
87–90	29.4	0	1.59	0	0	0	0	0	0	14.3	0	0
102–107	0	0	50	0	0	0	0	0	0	19.2	0	0
113–116	0	0	10.2	1.02	2.04	0	0	0	0	31.6	0	0
123–127	2.27	0	6.82	2.27	1.14	0	0	0	0	86.4	0	0
133–136	0	0	5.77	7.69	48.1	0	0	0	0	21.5	0	0
142–145	0	0	20.5	15.1	43.8	0.68	0	0	0	13.7	0	0
153–158	0	0	71.6	6.37	12.7	0	0	0.98	0	0	0.98	0
168–172	0	0	42.9	1.19	1.19	1.19	5.95	4.76	0	0	9.52	10.7
180–185	0	0	7.28	3.31	3.31	5.96	5.96	6.62	3.31	0	13.9	5.96
190–195	0	0	9.8	2.94	7.84	2.94	9.8	3.92	2.94	0	27.5	4.9

0–6	0	0	1.04	0	3.13	0	0	0	0	0	96
16– 18	0	0	0	0	3.85	0	0	0	0	0	286
26–29	0	0	0	0	0	0	2	4	0	0	50
34–36	0	0	2.13	0	0	0	0	0	0	0	47
46–49	0	0	44.6	0	0	0	0	0	0	0	56
51–54	0	0	86.3	0	0	0	0	0	0	0	95
66–69	0	0	44.4	0	0	0	0	0	0	0	27
81–84	0	0	58	0	0	0	0	0	0.89	0	112
87–90	0	0	46	0	0	0	0	3.17	5.56	0	126
102–107	0	0	0	0	0	0	0	0	30.8	0	52
113–116	0	0	0	0	0	0	0	3.06	52	0	98
123–127	0	0	0	0	0	0	0	0	0	0	88
133–136	0	0	0	0	0.38	0	0	0	0	0	260
142–145	0	0.68	0	0	0	0	0	0	0	0	146
153–158	0	0	0	0	0	0	0	0	0	0	204
168–172	0	5.95	0	2.38	0	1.19	0	0	0	0	84
180–185	0	1.32	0	5.3	0	3.31	0	1.99	0	2.65	151
190–195	0	3.92	0	0	0	0	0	0	0	2.94	102

Appendix F

Table A6
Ostracode species distribution in Core Ak 522, %

Depth, cm	*Cistacythereis rubra*	*Loxoconcha granulata*	*Loxoconcha lenta*	*Leptocythere devexa*	*Leptocythere bacescoi*	*Leptocythere sp.*	*Callistocythere diffusa*	*Xestoleberis aurantia*	*Xestoleberis cornelii*	*Cardona subellipsoida*	*Candona sp.*	*Paradoxostoma variabile*	*Cytheroma marinovi*	*Cyprinotus sp.*	*Gen. 1 sp.*	*Gen. 2 sp.*	*Gen. 3 sp.*	Total number of Ostracodes
20–25	26	3	49					10	6				5				1	175
30–33	51	8	27					7	3				0				4	73
40–43	18	4	67	1				0				1	7				2	212
50–53	25	5	65					0		1			2				2	130
60–63	15	23	46					0				3	8				5	39
69–72	13	61	7					0				4	13				2	54
80–83	0	69	10	1				0				1	15				4	168
90–93	1	74	4	1				0					17				3	138
100–103	0	81	3					0				1	14				1	184
110–113	7	79	4					0					7				3	157
119–125	38	58	1			1		0					0		1	1		111
135–139	7	93	0					0					0					30
150–153	10	65	0					19	6				0					31
156–158	11	36	0					38	15				0					39
168–170	37	13	0					50					0					8
175–179	23	9	0					59	9				0					22
188–191	54	41	0					0	5				0					22
191–195	39	10	0		4	2		41			2		2					51
200–203	36	14	0					43	7				0					14
209–210	40	12	0	8			4	24	12				0					25
212–214	52	1	0					43	4				0					69
214–216	40	11	0				3	20	15				0	11				35
221–224	62	0	0					24	14				0					21
226–229	53	0	0	5				35	7				0					40

Appendix G

Table A7
Ostracode species distribution in Core Ak 500, %

Depth, cm	*Cistacythereis aff rubra*	*Loxoconcha granulata*	*Leptocythere rara*	*Leptocythere aff bacescoi*	*Leptocythere lagunae*	*Leptocythere ramosa*	*Callistocythere adriatica*	*Xestoleberis aurantia*	*Bythocythere*	*Paradoxostoma*	*Pontocythere*	*Cytheridea*	*Senicytherura*	*Hirschmannia*	*Cytheroma variablis*	Other	Total number of ostracodes
0–2	14.8	29.6	0	11.1	0	0	3.7	0	0	0	25.9	3.7	0	0	11.1	0	27
9–11	12.5	50	0	25	0	0	0	0	0	0	0	0	0	0	12.5	0	8
14–16	8.7	78.3	0	4.35	0	0	0	0	0	0	0	4.35	0	0	0	4.35	23
24–26	42.1	50.9	0	1.75	0	0	3.51	0	0	0	1.75	0	0	0	0	0	57
34–36	20	60	0	0	0	0	0	0	0	0	20	0	0	0	0	0	5
44–46	23.7	64.5	0	3.95	0	0	1.32	0	0	1.32	1.32	1.32	0	0	0	0	76
49–51	25	39.5	0	2.63	0	0	3.95	0	1.32	1.32	25	0	0	0	0	1.32	76
54–56	30.9	53.6	0	4.12	0	0	6.19	0	0	0	1.03	4.12	0	0	0	0	97
64–66	22	58.5	0	4.88	0	0	0	0	0	0	9.76	0	2.44	0	2.44	0	41
69–71	12.5	71.9	0	6.25	0	0	3.13	0	0	0	0	0	0	3.13	3.13	0	32
79–81	5.56	70	0	2.22	0	0	1.11	0	0	6.67	0	2.22	1.11	0	11.1	0	90
89–91	19.5	72	0	0	0	0	1.22	0	0	2.44	3.66	0	0	0	1.22	0	82
99–101	18.8	79.2	0	0	0	1.04	0	0	0	0	0	0	0	0	1.04	0	96
114–116	19.6	69.6	0	0.98	0	0	9.8	0	0	0	0	0	0	0	0	0	102
124–126	17.5	71.1	0	2.06	0	6.19	0	0	1.03	1.03	0	0	0	0	1.03	0	97
134–136	8.6	65.6	0	10.8	0	12.9	0	0	0	0	0	0	0	0	2.15	0	93
139–141	0.65	40.5	0	19.6	0	7.84	1.31	0	0	0	0	0	0	0	29.4	0.65	153
144–146	0	39.6	0	20.8	0	35.4	0	0	0	0	0	0	0	0	4.17	0	48
154–156	1	56	1	3	18	14	1	0	0	3	0	0	0	0	3	0	100
159–161	0	24.1	0	22.6	0	11.3	0	0	0	0	0	0	0	0	42.1	0	133
199–200	27.6	70.1	0	0	0	0	0.38	1.92	0	0	0	0	0	0	0	0	261

Appendix H

Table A8
Ecological preference of benthic foraminiferal species according to (Michalevich, 1968; Yanko and Troitskaya, 1987; Yanko, 1989)

Species	Ecological preference
1. *Ammonia tepida* (Cushman, 1928) sin., dex.	Eurihaline 3–21‰, water depth 24–200 m, cold-water
2. *A. tepida* forma 1	
3. *A. tepida* forma 2	
4. *A. novoeuxinica* Janko, 1979	Eurihaline 2–19‰, water depth 7–56 m, rather cold-water
5. *A. compacta* (Hofker, 1969)	Polyhaline, ≥18–19‰, water depth 14–210 m, warm-water
6. *A. parkinsoniana* (d'Orbigny, 1839)	Polyhaline, warm-water
7. *Eggerella scabra* (Williamson, 1958)	Polyhaline, ≥18–19‰, water depth 14–210 m
8. *Cribroelphidium percursum* Janko, 1974	Polyhaline ≥18–19‰, water depth 13–185 m, warm-water
9. *Fissurina lucida* (Williamson, 1858)	Polyhaline ≥19–20‰, water depth 50–210 m, warm-water
10. *F. fragilis* Troitskaja, 1987	Polyhaline ≥18‰, water depth 50–210 m, warm-water
11. *F. porrecta* Troitskaja, 1987	Polyhaline ≥18–19‰, water depth 85–320 m, warm-water
12. *F. solida* Seguenza,	Polyhaline ≥18–19‰, water depth 58–220 m, warm-water
13. *Laryngosigma williamsoni* (Terquem, 1878)	Polyhaline ≥18–19‰, water depth 110–220 m, warm-water
14. *L. subulata* (Chapman et Parr, 1937)	Polyhaline, warm-water
15. *Esosyrinx jatzkoi* Janko, 1974	Polyhaline ≥19–20‰, water depth 36–185 m, warm-water
16. *Nonion matagordanus* Kornfeld,	Mesohaline, 11–19‰, water depth 10–220 m, warm-water
17. *N. pauciloculum* Cushman, 1944	Mesohaline, ≥11‰, water depth 35 m, warm–water
18. *Porosononion martcobi ponticus* Janko, 1989	Mesohaline, 11–21‰, water depth ~ 60 m, warm-water
19. *Aubignyna perlucida* (Heron — Allen et Earland, 1913)	Mesohaline, 11–21‰, water depth 7–10 m, cold-water
20. *A. tepida* forma *caucasica* (Janko, 1989)	Mesohaline, 11–21‰, water depth 10–70 m, warm-water
21. *A. tepida* forma *ammoniformis* (d'Orb., 1826)	Mesohaline, 11–21‰, water depth 5–220 m, warm-water
22. *Elphidium ponticum* (Dolgopolskaya et Pauli, 1931)	Mesohaline, 11–21‰, water depth 3–180 m, cold-water
23. *Quinqueloculina seminulum* (Linne, 1767)	Eurihaline 5–>21‰
24. *Florilus trochospiralis* Mayer, 1968	Oligohaline, cold-water.

Appendix I

Table A9
Depth preference of benthic foraminiferal species according to (Yanko and Troitskaya, 1987; Yanko, 1989)

Outer-shelf species (<35 M)	Inner-shelf species (35-70 M)	Deep-water species (70–250 M)
Ammonia tepida (Cushman, 1928) sin., dex.	*A. compacta* (Hofker, 1969)	*Fissurina lucida* (Williamson, 1858)
A. tepida forma 1	*Eggerella scabra* (Williamson, 1958)	*F. fragilis* Troitskaja, 1987
A. tepida forma 2	*Cribroelphidium percursum* Janko, 1974	*F. porrecta* Troitskaja, 1987
A. novoeuxinica Janko, 1979	*Nonion matagordanus* Kornfeld, 1939	*F. solida* Seguenza, 1862
A. parkinsoniana (d'Orbigny, 1839)	*Porosononion martcobi ponticus* Janko, 1989	*Laryngosigma williamsoni* (Terquem, 1878)
N. pauciloculum Cushman, 1944	*Aubignyna perlucida* (Heron — Allen et Earland, 1913)	*L. subulata* (Chapman et Parr, 1937)
A. tepida forma *caucasica* (Janko, 1989)	*A. compacta* forma *ammoniformis* (d'Orb., 1826)	*Esosyrinx jatzkoi* Janko, 1974
Quinqueloculina seminulum (Linne, 1767)	*Elphidium ponticum* (Dolgopolskaya et Pauli, 1931)	
Canalifera nigarensis (Cushman, 1939)	*Florilus trochospiralis* Mayer, 1968	

Appendix J

Table A10
Average values of carbon and oxygen isotope analyses of mollusk shells in Core Ak 521

Depth, cm	Midpoint, cm	Mollusk species	$\delta^{13}C$ vs PDB, ‰	$\delta^{18}O$ vs PDB, ‰
0–6	3,0	*Cardium exiguum*	1,058	0,597
20–22	21.0	–"–	1.190	0.317
24–26	25.0	–"–	0.326	0.491
29–31	30.0	–"–	0.608	0.832
31–34	32.5	–"–	0.528	0.707
74–76	75.0	–"–	0.705	0.210

(continued on next page)

Table A10 (*continued*)

Depth, cm	Midpoint, cm	Mollusk species	$\delta^{13}C$ vs PDB, ‰	$\delta^{18}O$ vs PDB, ‰
95–98	96.5	–"–	0.831	0.111
100–103	10.5	–"–	0.643	0.171
119–123	121.0	–"–	0.208	0.137
123–127	125.0	–"–	0.690	0.446
158–163	160.5	*Dreissena rostriformis*	0.533	−1.642
163–168	165.5	–"–	0.415	−1.946
168–172	170.0	–"–	0.410	−1.877
172–175	173.5	–"–	0.388	−2.232
0–6	3.0	*Modiolus phaseolinus*	0.718	0.337
8–11	9.5	–"–	1.116	0.747
11–14	12.5	–"–	1.608	0.684
14–16	15.0	–"–	1.964	0.923
16–18	17.0	–"–	1.235	0.814
18–20	19.0	–"–	1.658	0.807
20–22	21.0	–"–	1.728	1.029
24–26	25.0	–"–	1.825	0.723
36–39	37.5	*M. lineatus*	1.366	−0.017
39–41	40.0	–"–	1.503	−0.038
41–44	42.5	*Mytilus edulis*	1.273	−0.042
44–46	45.0	–"–	0.961	−0.152
49–51	50.0	–"–	1.350	−0.189
51–54	52.5	–"–	0.825	−0.030
54–56	55.0	–"–	0.963	−0.058
56–59	57.5	–"–	0.635	−0.066
59–62	60.5	–"–	1.122	−0.031
62–64	63.0	–"–	0.827	0.125
64–66	65.0	–"–	1.397	0.017
66–69	67.5	–"–	1.126	0.029
69–71	70.0	–"–	0.479	−0.060
71–74	72.5	–"–	1.045	−0.118
74–76	75.0	–"–	1.102	0.040
76–79	77.5	–"–	1.253	−0.181
79–81	80.0	–"–	1.948	−0.145
84–87	85.5	–"–	1.627	−0.063
87–90	88.5	–"–	1.578	−0.155
90–92	91.0	–"–	1.576	−0.216
92–95	93.5	–"–	1.487	−0.172
95–98	96.5	–"–	1.479	−0.164
100–103	101.5	–"–	1.734	−0.089
102–107	104.5	–"–	1.190	−0.338
107–110	108.5	–"–	1.860	−0.224
110–113	111.5	–"–	1.270	−0.196
113–116	114.5	–"–	1.719	−0.249
116–119	117.5	–"–	1.152	−0.114
119–123	121.0	–"–	1.600	−0.331
123–127	125.0	–"–	1.302	−0.070
127–130	128.5	–"–	1.926	−0.197
130–133	131.5	–"–	1.469	−0.177
133–136	134.5	–"–	1.889	−0.297
136–139	137.5	–"–	1.860	−0.383
139–142	140.5	–"–	1.671	−0.347
142–145	143.5	–"–	1.974	−0.350
145–148	146.5	–"–	1.673	−0.273
158–163	160.5	–"–	0.728	−0.404

Appendix K

Table A11
Average values of carbon and oxygen isotope analyses of mollusk shells in Core Ak 500

Depth, cm	Midpoint, cm	Mollusk species	δ^{13}C vs PDB, ‰	δ^{18}O vs PDB, ‰
24–26	25.0	*C. exiguum*	1.345	−0.031
44–46	45.0	–"–	1.593	−0.006
46–49	47.5	–"–	1.413	0.021
49–51	50.0	–"–	1.438	0.193
54–56	55.0	–"–	1.868	−0.193
64–66	65.0	–"–	1.706	−0.217
69–71	70.0	–"–	1.682	−0.006
79–81	80.0	–"–	1.457	−0.110
94–96	95.0	–"–	1.204	0.019
99–101	100.0	–"–	0.848	0.238
101–104	102.5	–"–	0.800	0.362
109–111	110.0	–"–	1.112	0.083
111–114	112.5	–"–	1.409	0.276
114–116	115.0	–"–	0.759	0.337
119–121	120.0	–"–	1.528	−0.152
129–131	130.0	–"–	1.236	0.461
199–200	199.5	–"–	0.738	0.340
44–46	45.0	*M. edulis*	1.565	−0.274
46–49	47.5	–"–	0.961	−0.004
54–56	55.0	–"–	1.687	−0.492
79–81	80.0	–"–	1.842	−0.671
99–101	100.0	–"–	1.301	−0.107
101–104	102.5	–"–	1.340	−0.008
111–114	112.5	–"–	1.705	−0.210
114–116	115.0	–"–	1.350	−0.370
144–146	145.0	–"–	1.017	0.061
199–200	199.5	–"–	1.276	−0.059

Appendix L. Supplementary data

Supplementary data associated with this article can be found, in the online version, at doi:10.1016/j.palaeo.2006.09.014.

References

Aksu, A.E., Hiscott, R.N., Mudie, P.J., Gillespie, H., Yasar, D., 2002. Last glacial–Holocene sea surface temperature and salinity variations in the Black and Marmara Sea: stable isotopic, planktonic foraminiferal and coccolith evidence. Mar. Geol. 190, 119–149.

Algan, O., Çağatay, N., Chepalyga, A., Ongan, D., Eastoe, C., Gökaşan, E., 2001. Stratigraphy of the sediment infill in Bosphorus Strait: water exchange between the Black and Mediterranean Seas during the last glacial Holocene. Geo-Mar. Lett. 20, 209–218.

Andrusov, N.I., 1965. *Izbrannie trudi* (Selected Publications) T. 4. Nauka, Moscow. (in Russian).

Arkhangelskii, A.D., Strakhov, N.M., 1938. Geologicheskoe Stroenie i Istoriya Razvitiya Chernogo Morya (Geological Structure and History of the Black Sea). Izdatelstvo Akademii Nauk SSSR, Moscow. (in Russian).

Arslanov, Kh.A., Balabanov, I.P., Gey, N.A., Izmailov, Ya.A., 1982. Methods and results of mapping and geochronological correlation of ancient shorelines of the Black Sea on its coast and shelf. In: Kaplin, P.A., et al. (Ed.), Fluktuatsii Urovnya Moray za Poslednie 15 tis. Let. (Sea Level Fluctuations During the Last 15 ka). Nauka, Moscow, pp. 144–150 (in Russian).

Bahr, A., Lamy, F., Arz, H., Kuhlmann, H., Wefer, G., 2005. Late glacial to Holocene climate and sedimentation history in the NW Black Sea. Mar. Geol. 214, 309–322.

Balabanov, I.P., Izmailov, Ya.A., 1988. Changes in level and hydrochemical regime of the Black Sea and the Sea of Azov during the last 20 ka. Vodn. Resur. 15, 539–546 (in Russian).

Ballard, R.D., Coleman, D.F., Rosenberg, G., 2000. Further evidence of abrupt Holocene drowning of Black Sea shelf. Mar. Geol. 170, 253–261.

Chepalyga, A.L., 2002. The Black Sea. In: Velichko, A.A. (Ed.), Razvitie Landshaftov i Klimata Severnoy Evrazii: Pozdniy Pleystocen–Golocen — Aspecti Buduschego. (Development of the Northen Eurasia Landscapes and Climate: Last Pleistocene–Holocene — Perspectives of the Future). GEOS, Moscow, pp. 205–285 (in Russian).

Chepalyga, A.L., Mikhailesku, K.D., Izmailov, Ya.A., Markova, A.K., Kats, Yu.I., Yanko, V.V., 1989. Problems of Pleistocene stratigraphy and palaeogeography of the Black Sea. In: Alexeev, M.N. (Ed.), Chetvertichniy Period: Stratigrafiya. (Quaternary Period: Stratigraphy). Nauka, Moscow, pp. 113–120 (in Russian).

Colalongo, M.L., Pasini, G., 1980. La Ostracofauna plio–pleistocenica della Sezione Vrica in Calabria (con considerazioni sul limite Neogene/Quaternario). Boll. Soc. Paleontol. Ital. 19 (1), 1–126 (in Italian).

Degens, E.T., Ross, D.A., 1972. Chronology of the Black Sea over the last 25,000 years. Chem. Geol. 10, 1–16.

Elliot, M., deMenocal, P.B., Linsley, B.K., Howe, S.S., 2003. Environmental controls on the stable isotopic composition of *Mercenaria mercenaria*: potential application to paleoenvironmental studies. Geochem. Geophys. Geosyst. 4 (7), 1056, doi:10.1029/2002GC000425, 16 pp.

Fairbanks, R.G., 1989. A 17,000-year glacio–eustatic sea level record: Influence of glacial melting rates on the Younger Dryas event and deep-ocean circulation. Nature 342, 637–642.

Fedorov, P.V., 1977. Poznechetvertichnaya istoriya Chernogo morya i razvitie yuzhnikh morey Evropy (Late Quaternary history of the Black Sea and development of the southern Europe seas). In: Alexeev, M.N. (Ed.), Paleogeographiya i Otlozjeniya Pleistocena Yuzhnikh Morey SSSR. (Pleistocene Palaeogeography and Sediments of the Southern USSR Seas). Nauka, Moscow, pp. 25–32 (in Russian).

Fedorov, P.V., 1978. Pleistotsen Ponto-Kaspiya. (leistocene of the Ponto-Caspian Region). Nauka, Moscow. (in Russian).

Fedorov, P.V., 1985. O kolebaniyah urovnya Chernogo moray v golotsene (On water-level fluctuations in the Black Sea during the Holocene). In: Alexeev, M.N. (Ed.), Geologiya I Geomorfologiya Shelfa I Kontinentalnogo Sklona. (Geology and Geomorphology of Shelves and Continental Slopes). Nauka, Moscow, pp. 131–136 (in Russian).

Gaffey, S.J., Bronnimann, C.E., 1993. Effects of bleaching on organic and mineral phases in biogenic carbonates. J. Sediment. Petrol. 63, 752–754.

Görür, N., Çağatay, N., Emre, Ö., 2001. Is the abrupt drowning of the Black Sea shelf at 7150 yr BP a myth? Ibid 176, 65–73.

Grossman, E.L., 1982. Stable isotopes in live benthic foraminifera from the Southern California Borderland. Ph. D. Dissertation, Univ. of Southern California. 164 pp.

Grossman, E.L., Betzer, P.R., Dudley, W.C., Dunbar, R.B., 1986. Stable isotopic variation in pteropods and atlantids from North Pacific sediment traps. Mar. Micropaleontol. 10, 9–22.

Hiscott, R.N., Aksu, A.E., Yasar, D., Kaminski, M.A., Mudie, P.J., Kostylev, V.E., McDonald, J.C., Isler, F.I., Lord, A.R., 2002. Deltas south of Bosphorus Strait record persistent Black Sea outflow to the Marmara Sea since ~10 ka. Mar. Geol. 190, 95–118.

Izmailov, Y.A., 2005. Evolutsionnaya geografiya poberejiy Tchernogo I Azovskogo morey. Evolutionary Geography of the Black Sea and Sea of Azov Coasts. T 1. (Anapa Sand Barrier). Lazarevskaya Polygrafiya, Sochi. 174 pp. (in Russian).

Kaplin, P.A., Selivanov, A.O., 2004. Lateglacial and Holocene sea level changes in semi-enclosed seas of North Eurasia: examples from the contrasting Black and White Seas. Palaeogeogr. Palaeoclimatol. Palaeoecol. 209, 19–36.

Keatings, K.W., Ito, E., Engstrom, D.R., Yu, Z.C., Heaton, T.H.E., Haskell, B.J., 1999. An investigation into the effect on ostracod shell chemistry of some chemical and physical cleaning techniques. Trans. - Am. Geophys. Union 80 (17), 176.

Kiliç, M., 2001. Recent Ostracoda (Crustacea) Fauna of the Black Sea Coasts of Turkey. Turk. J. Zoolog. 25, 375–388.

Kiseleva, M.I., 1981. Benthos Rikhlikh Gruntov Chernogo Morya (Benthos of the Black Sea Loose Soils). Naukova dumka, Kiev. (in Russian).

Lamy, F., Arz, H.W., Bond, G.C., Bahr, A., Patzold, J., 2006. Multicentennial-scale hydrological changes in the Black Sea and northern Red Sea during the Holocene and the Arctic/North Atlantic Oscillation. Paleoceanography 21 (1), PA1008, doi:10.1029/2005PA001184, 11 pp.

Livental, V.E., 1929. Ostracoda Akchagil'skogo i Apsheronskono Yarusov po Babazananskomu Razrezu (Ostracoda of the Akchagil and Apsheron Horizons along a Babazanan Profile). Izvestiya Azerbaijanscogo politekhnicheskogo instituta, Baku. (in Russian).

Major, C., Ryan, W., Lericolas, G., Hajdas, I., 2002. Constraints on Black Sea outflow to the sea of Marmara during the last glacial-interglacial transition. Mar. Geol. 190, 19–34.

Matthews, J.A., Briffa, K.R., 2005. The 'Little Ice Age': re-evaluation of an evolving concept. Geogr. Ann. 87 (1), 17–36.

Michalevich, V.I., 1968. Class Sarcoda. Opredelitel Fauni Chernogo i Azovskogo Morey. (The Faunal Key of the Black and Azov Seas). Naukova dumka, Kiev, pp. 9–21 (in Russian).

Mudie, P.J., Rochon, A., Aksu, A.E., 2002. Late Quaternary paleoclimatic and vegetation history of the Marmara–Black Sea region: land-sea correlation and paleoclimatic history. Mar. Geol. 190, 233–260.

Murdmaa, I.O., Ivanova, E.V., Levchenko, O.V., Merklin, L.R., Chepalyga, A.L., Lobkovskiy, L.I., Artemyeva, E.A., 2003. Postglacial events on north-eastern shelf of the Black sea. In: Laverov, N.P. (Ed.), Actualnie Problemi Oceanologii. (Relevant Problems of Oceanology). Nauka, Moscow, pp. 298–316 (in Russian).

Murdmaa, I., Polyak, L., Ivanova, E., Khromova, N., 2004. Paleoenvironments in Russkaya Gavan' Fjord (NW Novaya Zemlya, Barents Sea) during the last millennium. Palaeogeogr. Palaeoclimatol. Palaeoecol. 209, 141–154.

Myers, P.G., Wielki, C., Goldstein, S.B., Rohling, E.J., 2003. Hydraulic calculations of postglacial connections between the Mediterranean and the Black Sea. Mar. Geol. 201, 253–267.

Nevesskaya, L.A., 1965. Pozdnechetvertichniye Dvustvorchatie Molluski Chernogo Morya, ikh Sistematika i Ecologia (Late Quaternary Bivalvia of the Black Sea, their Systematics and Ecology). Nauka, Moscow. (in Russian).

Ostrovskii, A.B., Izmailov, Ya.A., Shcheglov, A.P., Arslanov, Kh.A., Tertichniy, N.I., Gey, N.A., Piotrovskaya, T.U., Muratov, V.M., Schelinskiy, V.E., Balabanov, I.P., Skiba, S.I., 1977. New data on Pleistocene stratigraphy and geochronology from marine terraces of the Caucasian Black Sea coast and Kerch–Taman region. In: Alexeev, M.N. (Ed.), Paleogeografiya i Otlozheniya Pleistocena Yuzhnikh Morey SSSR. (Pleistocene Palaeogeography and Sediments of the Southern USSR Seas). Nauka, Moscow, pp. 61–68 (in Russian).

Pasechnik I.V., 2003. Visokorazreshayuschaya stratigraphiya verkhnechetvertichnikh otlojeniy Kavkazskogo shelfa Chernogo morya po bentosnim foraminiferam. (Late Quaternary high-resolution stratigraphy of the Black Sea Caucasian shelf based on benthic foraminifera). MSc. Thesis. Moscow State University, Moscow (in Russian).

Ross, D.A., Degens, E.T., 1974. Resent sediments of the Black sea. The Black Sea: Geology, Chemistry and Biology. Okla, Tulsa.

Ryan, W.B.F., Pitman III, W.C., Major, C.O., Shimkus, K., Moskalenko, V., Jones, G.A., Dimitrov, P., Gorur, N., Yuce, H., 1997. Abrupt drowning of the Black Sea shelf. Mar. Geol. 190, 119–126.

Ryan, W.B.F., Major, C.O., Lericolais, G., Goldstein, S.L., 2003. Catastrophic flooding of the Black Sea. Ann. Rev. Earth Planet. Sci. 31, 525–554.

Sharp, Z., 2006. Principles of Stable Isotope Geochemistry. Pearson Prentice Hall, Upper Saddle River, NJ.

Shornikov, E.I., 1969. Subclass Ostracoda. Opredelitel Fauni Chernogo i Azovskogo Morey. (The Faunal Key of the Black and Azov Seas). Naukova dumka, Kiev, pp. 163–260 (in Russian).

Shornikov, E.I., 1972. Ecology problems of the Azov and the Black sea Ostracoda. Biologiya Morya. Vip. 26. Ecologicheskie Issledovaniya Donnikh Organizmov. (Marine Biology, V. 26.

Ecological Investigations of Benthic Organisms). Naukova dumka, Kiev, pp. 58–88 (in Russian).

Surge, D., Walker, K.J., 2006. Geochemical variation in microstructural shell layers of the southern quahog (*Mercenaria campechiensis*): implications for reconstructing seasonality. Palaeogeogr. Palaeoclimatol. Palaeoecol. 237, 182–190.

Uchupi, E., Ross, D.A., 2000. Early Holocene marine flooding of the Black Sea. Quat. Res. 54, 68–71.

Vander Putten, E., Dehairs, F., Keppens, E., Baeyens, W., 2000. High resolution distribution of trace elements in the calcite shell layer of modern Mytilus edulis: Environmental and biological controls. Geochim. Cosmochim. Acta 64 (6), 997–1011.

Yanko, V.V., 1982. The stratigraphy of a late Quaternary sediments in the Black sea north-eastern shelf on a benthic foraminifera. In: Juze, A.P., Krasheninnikov, V.A. (Eds.), Morskaya Micropaleontologiya. (Marine Micropaleontology). Nauka, Moscow, pp. 126–131 (in Russian).

Yanko V.V., 1989. *Chetvertichnie foraminiferi Ponto–Kaspiya:(klassificatsiya, ecologiya, biostratigraphiya, istoriya razvitiya)*. (Quaternary foraminifera of the Ponto–Caspian (classification, ecology, biostratigraphy, and evolution)). Dr. Sc. Thesis, Odessa State University, Ukraine (in Russian).

Yanko, V.V., Gramova, L.V., 1990. The stratigraphy of the Black Sea Caucasian shelf and continental slope Quaternary sediments on a microfauna. Sov. Geol. 2, 60–73 (in Russian).

Yanko, V.V., Troitskaya, T.S., 1987. Pozdnechetvertichnie Foraminiferi Chernogo Morya (Late Quaternary Foraminifera of the Black Sea). Trudi Institutageologii I Geofiziki SO AN SSSR, p. 694.